INVESTIGATION OF CELL MIGRATION AND PROLIFERATION IN AGAROSE BASED HYDROGELS FOR TISSUE ENGINEERING APPLICATIONS

A THESIS SUBMITTED TO
THE GRADUATE SCHOOL OF NATURAL AND APPLIED SCIENCES
OF
MIDDLE EAST TECHNICAL UNIVERSITY

BY

ELİF VARDAR

IN PARTIAL FULFILLMENT OF THE REQUIREMENTS
FOR
THE DEGREE OF MASTER OF SCIENCE
IN
BIOMEDICAL ENGINEERING

JULY 2010

Approval of the thesis:

INVESTIGATION OF CELL MIGRATION AND PROLIFERATION IN AGAROSE BASED HYDROGELS FOR TISSUE ENGINEERING APPLICATIONS

submitted by **ELİF VARDAR** in partial fulfillment of the requirements for the degree of **Master of Science in Biomedical Engineering Department, Middle East Technical University** by,

Prof. Dr. Canan Özgen _____
Dean, Graduate School of **Natural and Applied Sciences**

Prof. Dr. Zülfü Aşık _____
Head of Department, **Biomedical Engineering**

Prof. Dr. Nesrin Hasırcı _____
Supervisor, **Chemistry Dept., METU**

Prof. Dr. Vasıf Hasırcı _____
Co-Supervisor, **Biological Sciences Dept., METU**

Examining Committee Members:

Prof. Dr. Zuhal Küçükyavuz _____
Chemistry Dept., METU

Prof. Dr. Nesrin Hasırcı _____
Chemistry Dept., METU

Prof. Dr. Duygu Kısakürek _____
Chemistry Dept., METU

Assoc. Prof. Dr. Caner Durucan _____
Metallurgical and Materials Engineering Dept., METU

Assoc. Prof. Dr. Ayşen Tezcaner _____
Engineering Sciences Dept., METU

Date: 16.07.2010

I hereby declare that all information in this document has been obtained and presented in accordance with academic rules and ethical conduct. I also declare that, as required by these rules and conduct, I have fully cited and referenced all material and results that are not original to this work.

Name, Last name: Elif Vardar

Signature:

ABSTRACT

INVESTIGATION OF CELL MIGRATION AND PROLIFERATION IN AGAROSE BASED HYDROGELS FOR TISSUE ENGINEERING APPLICATIONS

Vardar, Elif

M.Sc. Department of Biomedical Engineering

Supervisor : Prof. Dr. Nesrin Hasırcı

Co-Supervisor: Prof. Dr. Vasıf Hasırcı

July 2010, 86 pages

Hydrogels are three dimensional, insoluble, porous and crosslinked polymer networks. Due to their high water content, they have great resemblance to natural tissues, and therefore, demonstrate high biocompatibility. The porous structure provides an aqueous environment for the cells and also allows influx of nutrients needed for cellular viability. In this study, a natural biodegradable material, agarose (Aga), was used and semi-interpenetrating networks (semi-IPN) were prepared with polymers having different charges, such as positively charged chitosan (Ch) and negatively charged alginate (Alg). Hydrogels were obtained by the thermal activation of agarose with the entrapment of Ch or Alg in the Aga hydrogel structures. Chemical composition of hydrogels were determined by ATR-FTIR examinations, mechanical properties of hydrogels were examined through compression tests, morphologies were confirmed by scanning electron microscopy (SEM) and confocal microscopy, thermal properties were evaluated by differential scanning calorimetry (DSC) and thermogravimetric analysis (TGA). Moreover, swelling ratios, water

contact angles and surface free energies (SFE) were determined. Cell proliferation and cell migration within these hydrogels were examined by using L929 fibroblast cell line. MTS assays were carried out to observe the cell proliferation on hydrogels. Confocal microscopy was used in order to examine the cell behavior such as cell attachment and cell migration towards the hydrogels. It was observed that addition of positively charged Ch into agarose increased the ultimate compressive strength (UCS), decreased elastic modulus (E), increased the thermal stability and hydrophobicity of the semi-IPN hydrogels. On the other hand, addition of negatively charged Alg into agarose decreased UCS, E, thermal stability and hydrophilicity. Cell-material interaction results showed that Aga hydrogels in tissue engineering applications was improved by adding different charged polyelectrolytes. Cell migration within Aga hydrogels was enhanced by adding Ch, and hindered by addition of Alg. Maximum cell proliferation and maximum penetration of the cells were obtained with the Ch/Aga hydrogels most probably due to attraction between the negatively charged cell surface and the positively charged Ch/Aga hydrogel surface. It was shown that cell interaction of agarose hydrogel scaffolds could be enhanced by introducing chitosan within the agarose hydrogels and obtained structures could be candidates for tissue engineering applications.

Keywords: Hydrogel, Agarose, Chitosan, Alginate, Characterization, Cell proliferation, Cell migration.

ÖZ

DOKU MÜHENDİSLİĞİ UYGULAMALARI İÇİN AGAROZ BAZLI HİDROJELLERDE HÜCRE HAREKETİNİN VE ÇOĞALMASININ İNCELENMESİ

Vardar, Elif

Yüksek Lisans, Biyomedikal Mühendisliği

Tez Yöneticisi: Prof. Dr. Nesrin Hasırcı

Ortak Tez Yöneticisi: Prof. Dr. Vasıf Hasırcı

Temmuz 2010, 86 Sayfa

Hidrojeller üç boyutlu, çözünemeyen, gözenekli yapıda, çapraz bağlı polimerlerdir. Yüksek su tutabilme özelliklerinden dolayı, doğal dokularla oldukça benzerlik gösterirler ve bu nedenle biyouyumlulukları yüksektir. Gözenekli yapısı çözünmüş maddelerin ve hücre canlılığı için gerekli besinlerin akışını sağlar. Bu çalışmada, doğal ve biyobozunur bir malzeme olan agaroz (Aga) kullanılmış ve artı yüklü kitozan ve eksi yüklü aljinat (Alg) gibi farklı yüklere sahip diğer polimerler kullanılarak yarı geçişmiş ağ yapı şeklinde hidrojeller (semi-IPN) hazırlanmıştır. Hidrojeller, kitozan ve aljinatın agaroz içerisinde agarozun termal aktivasyonu sonucunda tutuklanmasıyla elde edilmiştir. Hidrojellerin kimyasal yapıları ATR-FTIR ile belirlenmiştir, hidrojellerin mekanik davranışları basma dayanımı testleriyle gözlenmiştir, morfolojileri taramalı elektron (SEM) mikroskobu ve konfokal mikroscobu ile incelenmiş, termal özellikler diferansiyel taramalı kalorimetre (DSC) ve termal ağırlık analizi (TGA) ile yapılmıştır. Ayrıca, hidrojellerin şişme yüzdeleri, temas açısı ve yüzey enerji ölçümleri yapılmıştır. Hücre çoğalması ve hidrojeller

içindeki hücre göçü çalışmaları L929 fibroblast hücre hattı kullanılarak yürütülmüştür. Hidrojeller üzerinde hücre çoğalma değeri MTS ölçümleri ile belirlenmiştir. Hidrojel yapılara hücre yapışması ve hücre difüzyonu gibi hücre davranışlarını incelemek için konfokal mikroskop kullanılmıştır. Agaroz hidrojellere pozitif yüklü Ch eklenmesi ile, maksimum basma dayanımının (UCS) arttığı, elastik modülünün (E) düştüğü, termal dayanıklılığının ve hidrofobikliğinin arttığı gözlemlenmiştir. Diğer taraftan, agaroz hidrojellere negatif yüklü Alg eklenmesi maksimum basma dayanımını (UCS), elastik modülünü (E), termal dayanıklılığı ve hidrofilikliği azaltmıştır. Hücre-malzeme etkileşimi sonuçları, agaroz hidrojelleri içerisine farklı yük yoğunluklarının eklenerek, bu hidrojellerin doku mühendisliği uygulamalarında kullanımının geliştirilebileceğini göstermiştir. Aga hidrojelleri içerisindeki hücre hareketi Ch eklenmesiyle artmış, Alg eklenmesiyle azalmıştır. Maksimum hücre göçü ve maksimum hücre çoğalması, büyük olasılıkla negatif yüklü hücre yüzeyi ve pozitif yüklü Ch/Aga hidrojellerinin elektrostatik etkileşiminden dolayı, Ch/Aga hidrojelleri üzerinde gözlemlenmiştir. Bu çalışmada, agaroz hidrojel destek yapılarının hücre etkileşiminin, agaroz hidrojellere kitozan eklenmesiyle geliştirilebilineceği ve elde edilen yapıların doku mühendisliği uygulamaları için uygun yapılar olabileceği gözlenmiştir.

Anahtar Kelimeler: Hidrojel, Agaroz, Kitozan, Aljinat, Karakterizasyon, Hücre çoğalması, Hücre hareketi.

To my precious family...

ACKNOWLEDGEMENTS

I would like to express my gratitude to my supervisor Prof. Dr. Nesrin Hasırcı for her valuable advice, continuous guidance, and encouragement and giving me a chance to be a part of her highly qualified laboratory throughout my study. I am deeply thankful for her motivation and support to complete this thesis.

I would like to express my deep appreciation to Prof. Dr. Vasıf Hasırcı for enlightening my professional and academic vision with his support, leadership and guidance. I am also thankful for making me a member of BIOMAT group that gave me the possibility of joining many international academic organizations supported by this team.

I am grateful to Prof. Dr. Michel Vert and his lab team for their support during my short visit to CNRS Research Center of Macromolecular Biochemistry in Montpellier, France.

My sincere acknowledgements go to Tuğba Endoğan and Aysel Kızıltay for their great patience, support, help and friendship as great lab partners. I am also thankful to them for their patience and help in microscopic examinations and for their guidance in cell culture tests. I wish to thank to all BIOMAT group members and Biotechnology Research Unit for providing us with contact angle measurements and cell culture tests. I am also thankful to my dearest lab partner Cansel Işıklı for her valuable friendship and moral support all through any time in my life.

I would like to thank to my dear friends Serkan Özçifçi, Ebru Koçak, Balam Balık, Elçin Yılmaz, Senem Gökçe Okullu, Bahar Acu, Gökhan Bulut and Onur Aktaş for

their precious friendship and support in every part of my life. They all have always been there for me.

This study was supported by METU-BAP 07-02-2009-00-01 and Tubitak Nano-Biomat project TBAG (105T508) and Tubitak 108T805 project; and these grants are gratefully acknowledged.

Finally, I would like to give special thanks to my father Maruf Vardar, my mother Birsen Vardar, my dear sister Ezgi Vardar for their encouragement, patience, and endless love they have shown through out all my life.

TABLE OF CONTENTS

LIST OF TABLES

TABLES

LIST OF FIGURES

FIGURES

ABBREVIATIONS

γ	Surface Tension
θ	Contact Angle
μ-CT	Micro Computed Tomography
2D	Two Dimensional
3D	Three Dimensional
Ch	Chitosan
DAPI	4', 6-Diamidino-2-Phenylindole
DMEM	Dulbecco's Modified Eagle Medium
DIM	Diiodomethane
DMSO	Dimethyl Sulfoxide
DSC	Differential Scanning Calorimetry
DW	Deionized Water
E	Rigidity (Young's Modulus)
ECM	Extracellular Matrix
FA	Formamide
FBS	Fetal Bovine Serum
FTIR-ATR	Fourier Transform Infrared-Attenuated Total Reflectance
GAG	Glycosaminoglycan
MTS	3-(4,5-dimethylthiazol-2-yl)-5-(3-carboxymethoxyphenyl)-2-(4-sulfophenyl)-2H-tetrazolium
NaOH	Sodium Hydroxide
PBS	Phosphate Buffered Saline
PFA	Paraformaldehyde
SEM	Scanning Electron Microscope
SFE	Surface Free Energy

TGA	Thermogravimetric Analysis
T_g	Glass Transition Temperature
UCS	Ultimate Compression Strength

CHAPTER 1

INTRODUCTION

1.1 Tissue Engineering

Tissue replacement or transplantation is one of the solutions to major health issues all over the world since lists of people waiting for organ transplants continuously areincreasing in every year [Tian et al., 2010; Sharma et al., 2010]. Before the mid-1980s, the gold standard for tissue repair was transplantation from the same person (autolograft), from the same species (allograft) or from a different species (xenograft) [Revell et al., 2009]. The first human renal transplantion surgery was performed successfully in 1954 by Dr. Joseph Murray who won Nobel prize in physiology in 1990. However, limited availability of donor tissues, post-operative donor site pain, the transmission of the diseases and immune reactions are the major limitations of tissue transplantation [Langer et al., 1993].

Scientists are interested in mimicking the natural body parts, and using the structures and organisms in nature as models. Tissue engineering has developed as an interdisciplinary field which combines engineering and life sciences and presents a potentially effective method to restore, maintain and improve the functions of tissue. The first tissue engineering concept was proposed in the United States in the 1981 to solve the donor problem. Connor et al. first reported the use of cultured epithelial grafts for the treatment of major burns, which could be counted as the first step for the usage of tissue engineering methods [Connor et al., 1981]. Tissue engineering deals with the production of tissues in the laboratory environment, in vitro conditions, by using some scaffolds and cells. Addition of bioactive agents

such as growth factors or hormones enhances the formation of tissues. Scaffolds should have the properties of a biomaterial.

Biomaterial is defined as the material used to replace or displace part of a living system which is not functioning properly or to help the biological system in contact with living tissue. Tissue engineering constitutes the most appropriate and fuctional biomaterial for any part, tissue or organ in the body for subsequent healing process [Hasirci et al., 2006]. In the production of engineered tissues several steps have to be taken into consideration [Langer et al., 1997]:

i) Selection of the most appropriate biomaterial, in the form of 2D or 3D scaffolds in order to support the detected area and promote healing,
ii) Selection of the most appropriate method for scaffold design in order to mimic in vivo environment of the native extracellular matrix (ECM) supported by bioactive agents such as growth factors,
iii) Selection of the proper cell type to be loaded within the scaffold.

1.2 Scaffold Materials and Types

The past decade has brought tremendous progress in artifical organs and use of both novel synthetic or natural materials for tissue engineering applications. Scaffolds provide a suitable mechanical and biological environment during new tissue formation when cells produce their own extracellular matrix (ECM). They are typically porous and biodegradable biomaterials [Gomes et al., 2004] and provide a support for cell attachment, differentiation, migration, modify cellular response over time and are designed so that they allow release of growth factors and drugs [Silva et al., 2009; Basmanav et al., 2008].

Scaffold materials used in tissue engineering applications can be derived from either synthetic or natural sources. Polylactides (PLA) [Tsourapas et al., 2006; Yucel et al., 2010], polyglycolides (PGA) [Kim et al., 2008; Kempen et al., 2008], and their copolymers such as poly(lactic acid)-co-glycolic acid (PLGA) [Wan et al., 2004; Hasirci et al., 2010], polycaprolactone (PCL) [Cao et al., 2003; Yilgor et al.,

2008] polyanhydrides [Tamada et al., 1992; Kumar et al., 2002], polyesters (PEG) [Inada et al., 1995; Tessmar et al., 2007] are the most popular synthetic polymers used as scaffold material partially due to the ease of their availability and degradability [Vogt et al., 2002].

Natural and naturally derived polymers are of special interest since they have biological and chemical similarities to natural tissues. Proteins such as gelatin [Ulubayram et al., 2005; Kosmala et al., 2000], collagen [Kose et al., 2004; Kinikoglu et al., 2009], elastin [Parks et al., 1993; Kielty et al., 2002] which are the main components of ECM and silk [Wang et al., 2006], polysaccharides such as chitosan [Berger et al., 2004], alginate [Rowley et al., 1999; Wang et al., 2003], agarose [Gruber et al., 2006], starch [Fuchs et al., 2009], are naturally derived biomaterials used as scaffold material.

Depending on the purpose (position and the shape of the implant site) scaffolds can be formed as the 2D (as film) or 3D (as fibrous, foam, sponge) porous structures. Since the architecture of a scaffold governs cell adhesion, spreading and orientation, the fabrication method of a scaffold should be selected according to the tissue and the place of the defect site. For instance, Kenar et al. (2010) was proposed that the effect of alignments of patterns on mesenchymal stem cells proliferation and differentiation on micro patterned poly(3-hydroxybutyrateco-3-hydroxyvalerate) (PHBV) and poly(L-D,L-lactic acid) (P(L-D,L)LA) blend films were quite significant [Kenar et al., 2010].

There are different techniques for scaffold fabrication. When the aim is to obtain a dense layer like a film, solvent casting is the method of choice. In order to obtain 3D scaffolds such as fiber, foam or sponge, phase separation/emulsion [Schugens et al., 1996], freeze drying [Whang et al.,1995; Mandal et al., 2009], electrospinning [Kenar et al., 2010], molecular imprinting [Tunc et al., 2006], membrane lamination [Mikos et al., 1993], melt molding [Se et al., 2006], gas foaming [Almirall et al., 2004] and rapid prototyping (RP) [Yeong et al., 2004; Yilgor et al., 2009] are widely employed scaffold fabrication techniques. Among these methods, RP is a powerful technique, especially if interconnected pores are

desired. RP based hydrogel scaffold fabrication using 3D plotting of thermoreversible gels were studied by Landers et al (2002), and this research is one of the pioneering studies for fabricating hydrogels by using rapid prototyping methods in the literature [Landers et al., 2002]. Although synthetic polymers seem to be more suitable for RP of scaffolds, some natural polymers such as chitosan, agarose and collagen [Maher et al. 2009; Norotte et al., 2009] have been used for producing hydrogels with predefined structures.

Hydrogels are one of the most fascinating scaffold options because of their high water content and their permeability to small molecules like oxygen, nutrients, and metabolites similar to natural tissue. Thus, they have considerably wide variety of applications in the area of tissue engineering.

1.3 Hydrogel Based Scaffolds

Hydrogels are 3D hydrophilic polymer networks and one of the promising scaffold options of tissue engineering due to their similarity to the extracellular matrix of soft tissues with their high water content. The porous structure creates available surfaces for cells to attach and also allows for the influx of nutrients needed for cellular viability and the transport of cellular waste out of the hydrogel. This high solute permeability allows them to be ideal materials for the controlled release of many drugs and other active agents as well as achieving 3D organization of cells for engineered tissues [Huang et al., 2006]. Moreover, the mechanical properties of hydrogels are quite similar to soft tissues so that appropriate structural growth cues can be received by the cells within the hydrogels. Also, the elasticity and water content of hydrogels can be tailored easily by controlling the crosslink density [Nisbet et al., 2008].

One of the first studies on biomedical hydrogels was reported in 1960 by Wichterle and Lim. They prepared a hydrogel based poly(2-hydroxyethyl methacrylate) and used it as a synthetic, soft contact lens material [Witcherle et al., 1960]. Since then, hydrogel based biomaterials have been a point of growing

interest in biomedical and tissue engineering applications. Some hydrogels and their biomedical application areas are summarized in Table 1.

Table 1 Biomedical applications of hydrogels.

Biomedical Application	**Polymer**	**Reference**
Contact lenses	PHEMA	Maldonado et.al., 2006
Blood compatible devices	PEG, PEGME, PHEMA, PVA, PEO, PAAm	Lin et.al., 2006; Faxälva et.al., 2010
Articular Cartilage, Artificial Skin	PVA, PHEMA Gelatin Collagen	Ramakrishna et.al., 2001 Schmedlen et al., 2002
Artificial Tendon	PHEMA, PTFE	Baidya et.al., 2003 Desai et.al., 2008
Drug Delivery Enzyme immobilization	PLA, PGA, Chitosan, Dextran,	Berger et.al., 2004 Serra et.al., 2009
Artificial Cartilage Gel Encapsulate Cells Wound dressings	Agarose, Alginate, Hyaluronic Acid, Chitosan	Sen et.al., 2005 Eisenbarth et al., 2007 Sakai et.al., 2007 Chou, et al., 2009

Hydrogels consist of reversibly or irreversibly crosslinked polymers and are prepared using several crosslinking methods. Two broad classifications can be made, namely physical and chemical crosslinking. In physical crosslinking, physical interactions between different polymer chains prevent dissolution and they are reversible. In chemical crosslinking, polymer chains are bonded to each other with ionic or strong covalent bond where the covalent linkage is irreversible. Physical crosslinking methods are widely used for preparing hydrogels due to the absence non-toxic crosslinking agents [Nickerson et al., 2006]. Reversible crosslinkings can

be made by means of ionic interactions, hydrogen bonds, protein interactions or crystallization. Physical crosslinking might enable the system to dynamically respond to external stimuli such as temperature, pH, and mechanical loading. Alginate is a well known polymer which can form gels by ionic interactions. Figure 1 shows the crosslinking of alginate with Ca^{+2} ions.

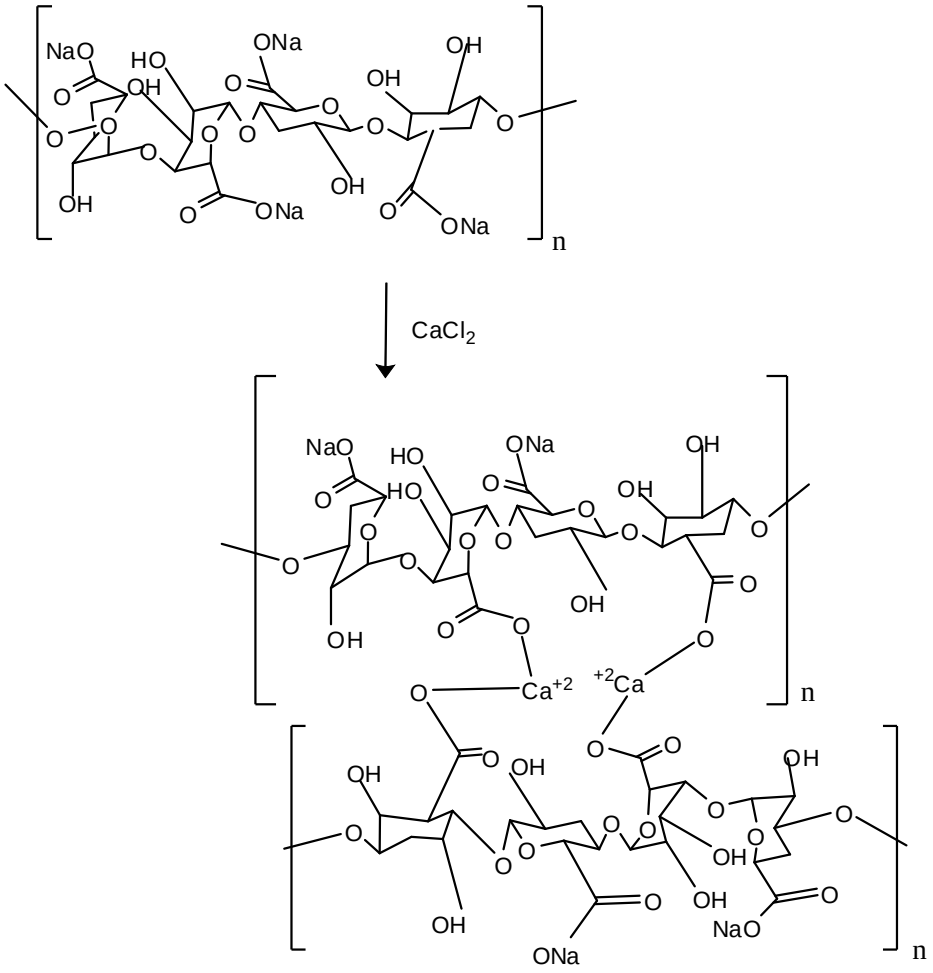

Figure 1 Crosslinking mechanism of alginate.

Chemical crosslinking involves strong covalent bonds which maintain the integrity of the structure between polymer chains. Radical polymerization, high

energy irradiation, chemical reactions of complementary groups and using enzymes are the most important ways of chemical crosslinking. In this type of crosslinking, irreversible chemical links are formed [Liu et al., 2007] and these covalent inteactions lead to the formation of a permanent network and enhancing the mechanical properties of the gel and allowing the diffusion of water. However, ionic crosslinking creates non-permanent networks which have reversible links; these hydrogels might enable cell diffusion or higher swelling ratios. Main drawbacks of chemical crosslinks are the toxicity of residual covalent crosslinkers [Zan et al., 2006]. Figure 2 shows the crosslinking mechanism of chitosan in the presence of glutaraldehyde.

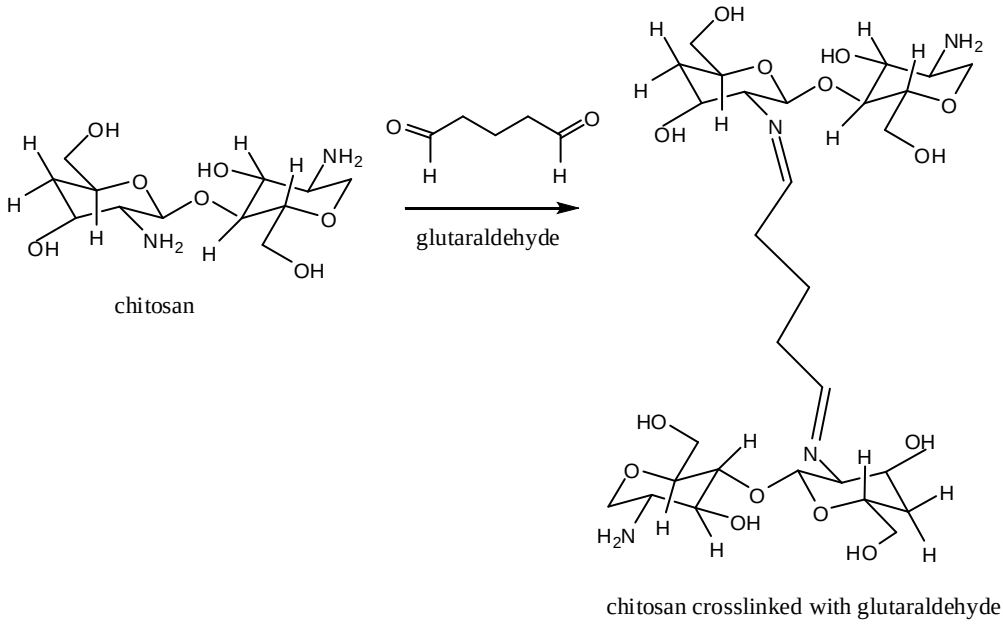

Figure 2 An example of chitosan crosslinking mechanism with glutaraldehyde.

The application areas of hydrogel scaffolds are influenced significantly by their swelling properties. The swelling ratio of hydrogel is a critical parameter since it shows the amount of water that is contained within the hydrogel at equilibrium. To determine the swelling of hydrogels, vacuum-dried hydrogel samples are immersed into the prepared physiological solutions and the weight changes in

different time intervals are recorded. Molecular weight of the chains between the crosslinks, pH of solution, and temperature considerably affect swelling ratio of hydrogels [Kim et al., 2003]. High swelling capacity of hydrogel scaffolds is also depended on high ratio of ionizable groups. The presence of the ionic groups in polymer chains results an increase in swelling because the ions are more strongly solvated rather than non-ionic groups in the aqueous medium [Mahdavinia et al., 2004].

Photopolymerizable hydrogels are used in many tissue engineering applications, including bone, cartilage, and vascular tissues [Schweitzer et al., 2009; Tan et al., 2008]. Photocrosslinking enables the polymers to be gelled in situ. By controlling UV exposure duration, photoinitiator concentration, monomer chain length, and conjugation of biological molecules, gel properties can be easily tailored.

Another classification of hydrogel preparation is the type of polymer used; homopolymer hydrogels (one type, hydrophilic), copolymer hydrogels (two types of monomer, at least one hydrophilic), multimonomer hydrogels (more than three types of monomer) and interpenetrating polymeric hydrogels (network formed by intermeshing of a polymer in another) can be used in tissue engineering applications.

By proper design of hydrogels it is possible to control the kinetics of delivery of active ingredients or to control tissue regeneration by enabling micro and macro-environment for cells to attach and grow. Thus, by using appropriate preparation techniques of hydrogels, desired scaffold designs can be achieved. For this reason, much of the research on hydrogels has been focused on how different crosslinking methods affect the properties of the hydrogel scaffolds [Park et al., 2009; Sheikh et al., 2010].

Interpenetrating polymeric hydrogels are highly desirable for tissue engineering applications. Interpenetrating network (IPN) consists of two crosslinked polymers. When only one of them is crosslinked while the other is in linear form, the network is called semi-IPN.

Hydrogels can be further classified based on their structures; amorphous hydrogels (chains randomly arranged), semicrystalline hydrogels (some regions are ordered macromolecules, some of them randomly arranged) and hydrogen-bonded hydrogels. According to responsiveness towards stimuli physical properties, hydrogels can be divided into conventional and responsive hydrogels. The first group is lightly crosslinked and it swells in water limited by their chemistry and crosslinking degree. They exhibit no changes with external stimuli such as pH, temperature, light, etc. and are usually uncharged. The responsive hydrogels exhibit volume change in response to stimuli and they usually contain an important hydrophobic component [Rosiak et al., 1999; Chaoliang et al., 2008]. Hydrogels in this group are further held together by molecular entanglements, and/or secondary forces such as ionic or H-bondings or by hydrophobic interactions. For instance, agarose forms thermoreversible gels which show coil to helix transition during cooling. Figure 3 shows this transformation [Rees et al., 1969].

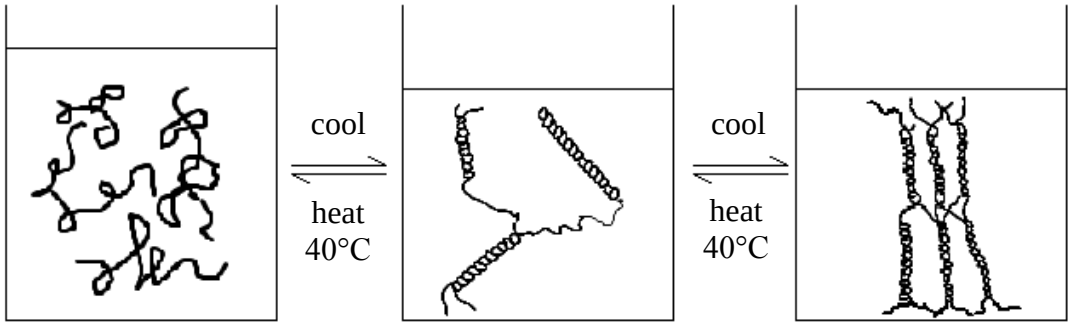

Figure 3 Coil to helix transition of agarose during gelation.

Another important way of classification is based on the constituents of hydrogels; these hydrogels can be made of either synthetic or natural polymers. In the following section, these types are discussed in detail.

1.3.1 Synthetic Polymer Based Hydrogels

A variety of synthetic polymers can be used to produce hydrogel scaffolds for tissue engineering applications since their chemistry and properties are controllable and reproducible. Methacrylate-based hydrogels are commonly used materials especially for neural tissue engineering due to their similarity of mechanical properties to the natural tissue. The main polymer type in this class is poly(2-hydroxyethyl- methacrylate) (pHEMA) due to its ease of modifications with molecules such as adhesive protein-derived oligopeptides or collagen [Yu et al., 2005]. There are numerous studies of using pHEMA based hydrogels such as injectable matrix, implants [Filmon et al., 2000], drug delivery [Chouhan et al., 2009] and scaffolds for bone tissue engineering [Costa et al., 2003].

Another important synthetic polymer is polyethylene glycol (PEG) which is a hydrophilic polymer used in drug delivery, as surgical barrier, cell encapsulation for transplantation, and as scaffolds in cartilage tissue engineering [Pfister et al., 2007]. PEG-based hydrogels have FDA approval in human intravenous, oral and dermal applications and another property of them is that their conjugation to proteins prevents recognition by the immune system and this increases biocompatibility [Fee et al., 2006].

Both PEG and polyethylene oxide (PEO) are almost identical and can be photocrosslinked after modifying each end of the polymer with either acrylate or methacrylates [Mann et al., 2001].

Other examples of synthetic polymers for hydrogel fabrication include polyvinyl alcohol (PVA) [Wang et al., 2006; Yanpeng et al., 2006], and poly(N-isopropylacrylamide) P(NIPAM) [Ozturk et al., 2009]. Among these polymers, P(NIPAM) is a well known thermoresponsive polymer with a lower critical solution temperature (LCST) of around 32°C in aqueous medium [Simonid et al., 2007]. For this reason, its hydrogels shrink above, and swell below 32°C [Matsuyama et al., 1991]. This property can be used for the on-demand release of drugs, separation of

the aqueous solution of proteins and immobilization of enzymes and cells [Nakamura et al., 2004; Wang et al., 2008].

1.3.2 Natural Polymer Based Hydrogels

Naturally derived materials have fascinating properties such as their similarities to the extracellular matrix as polysaccharides and glycosaminoglycans (GAGs). They can be degraded by naturally occurring enzymes. Furthermore, in some cases, they send appropriate signals to cells without the need for growth factors. Most of these materials have very similiar mechanical properties when they are processed and they can support the tissue like the natural extracellular matrix (ECM) and they provide optimal microenvironment for cell adhesion and tissue in-growth. In the literature, numerous studies were dedicated to naturally derived hydrogels such as collagen, gelatin, hyaluranate, agarose, alginate and chitosan. Collagen is a very well known as it is the most abundant protein of ECM in mammalian tissues. Collagen is composed of three polypeptide chains, which wrap around one another to form a three-stranded structure and these strands which can self aggregate to form stable fibers are held together by both hydrogen and covalent bonds [Lee et al., 2001]. Collagen hydrogels can be formed by chemical crosslinks (e.g. glutaraldehyde, formaldehyde, carbodiimide) or by physical treatments (e.g. UV irradiation, lyophilization, heating) [Lee et al., 2001; Park et al., 2002].

Gelatin is derivative of collagen whose triple helix is broken into simple strands. It is the major constituent of human bone and skin and also animal extracellular matrix [Buckwalter et al., 2005]. Gelatin has its arginine-glycine-aspartine (RGD) sequence that promotes the initial cell adhesion on the gelatin based scaffolds [Rohanizadeh et al., 2008]. Both, negatively charged acidic gelatin and positively charged basic gelatin (at physiological pH) can be obtained since isoelectric point of gelatin can be modified. This modification allows electrostatic interactions between a charged biomolecule and charged gelatin to form polyion

complexes [Djagny et al., 2001]. Gelatin based hydrogels are water soluble if not covalently crosslinked. For this reason, they should be crosslinked and generally glutaraldehyde or carbodiimide are used for this purpose by forming amide bonds. Because of their promising properties, both gelatin and collagen have been used in controlled release of growth factors, delivery of cells, and as scaffolds especially for tissue engineering of skin. Hyaluronan (hyaluronic acid) (HA) is a member of GAG family found naturally in the ECM of humans. It is a negatively charged polysaccharide and is comprised of alternating glucuronic acid and N-acetylglucosamine units. HA is reported to promote nerve regeneration in peripheral nerve conduits, wound healing, drug delivery, and in corneal implants [Merrett et al., 2008]

The structural properties of agarose, alginate and chitosan biopolymers, and their hydrogel applications will be discussed in more detail in the following sections, since these polymers and hydrogels prepared from these polymers were studied in this research.

1.3.2.1 Agarose

Agarose (Aga) is a natural and neutral polysaccharide from marine red algae [Aymard et al., 2001]. It forms three dimensional thermoreversible gels by thermal activation consisting of repeating units of alternating β-1,3 linked D-galactose and α-1,4 linked 3,6 anhydro-α L-galactose residues (Figure 4).

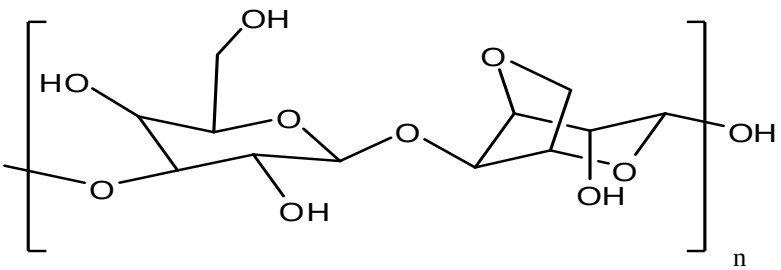

Figure 4 Repeating unit of agarose.

As explained in section 1.3, agarose can undergo coil-helix transition and the helices lead to conversion of a more ordered structure of agarose through hydrogen bonds [Rees et al., 1969]. This conversion makes agarose hydrogels concentration and temperature dependent, and also affects its mechanical properties [Buckley et al., 2009]. In the literature, agarose is widely used in nerve regeneration applications, such as artificial tubular nerve guidance channels [Dodla et al., 2008] and injectable nerve guide systems [Willerth et al., 2007]. This is due to its supporting neurite extension in a non-immunogenic manner. Injectibility is a result of the ability to solidify naturally at low gelation temperature, around 35°C, very close to the body temperature [Sakai et al., 2007].

Besides neural tissue engineering applications, agarose gels are widely used in pharmaceutics [Bica et al., 2001], thickening and stabilizing food systems [Meena et al., 2009], drug delivery devices [Liang et al., 2006], in dentistry in the production of intricate casts [Moioli et al., 2000], encapsulation of cells (islets of Langerhans, chondrocytes, etc.) [Rinaudo et al., 2008], artificial cartilage engineering [Schulz et al., 2006] and wound healing [Rinaudo et al., 2008]. Like other temperature sensitive hydrogels, agarose exhibits LCST at 35°C, below which the hydrogel can be swollen, hydrated and hydrophilic, and above it, the gel becomes collapsed, dehydrated and hydrophobic [Goycoolea et al., 2007]. This process is fully reversible, in other words, the soluble and gel states can be reversibly transformed into each other many times without any change in polymer properties. However, various studies claim that agarose hydrogels do not support cell proliferation enough because agarose does not contain any cell adhesive amino acid sequences in itself [Sakai et al., 2007]. For this reason, modification of agarose with peptides containing cell recognition motifs such as RGD and blending agarose with charged polymers have started gaining much attention for enhancing cell interaction to agarose.

1.3.2.2 Chitosan

Chitosan (Ch) is a natural, semicrystalline and positively-charged polysaccharide obtained by NaOH treatment of chitin at 120°C for 1-3 h that produces at least 70% deacetylated chitosan (Figure 5). Chitosan is a linear polymer of β-(1-4) linked D-glucosamine residues with N-acetyl-glucosamine groups.

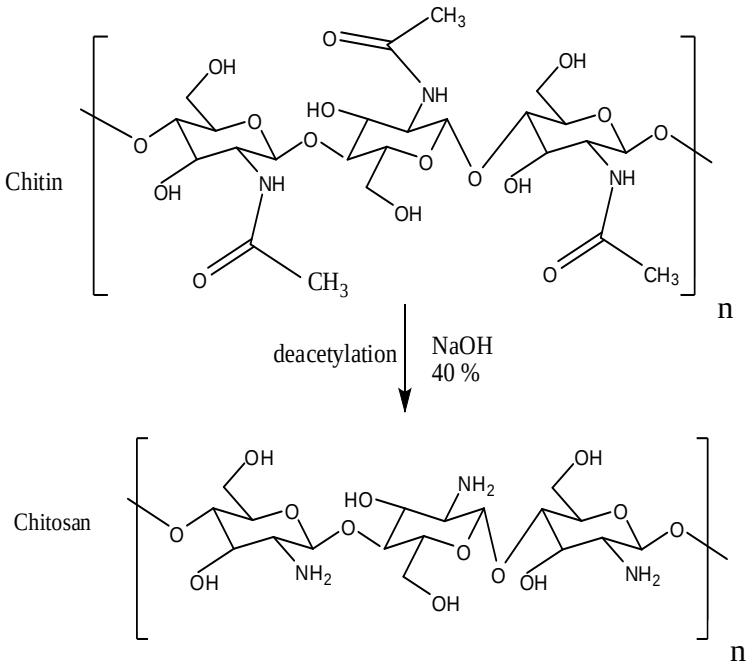

Figure 5 Chemical structure of chitin and chitosan.

Characteristics of chitosan are mainly influenced by its molecular weight (MW) and its degree of deacetylation (DD). At least 80% deacetylated chitosan is soluble in dilute acids because of protonation of amino groups [Dornish et al., 2001]. Its natural and general biocompatibility leads to its use in biomedical area as a biological adhesive for soft tissues [Ono et al., 2000], wound healing agent [Berger et al., 2004], drug delivery device for controlled release of bioactive agents as membrane for dialysis [Prabaharan et al., 2004], coatings [Rinaudo et al., 2008],

dialysis membrane [Rinaudo et al., 2008], enzyme immobilization system [Rinaudo et al., 2008], cell encapsulation material [Vieira et al., 2008], and antimicrobial agent [Zivanovic et al., 2007, Sarasam et al., 2008].

Both blending of chitosan with other polymers and crosslinking are effective methods for improving its physical and mechanical properties as well as widening its application area [Lin-Gibson et al., 2003]. Various crosslinkers such as glutaraldehyde [Mourya et al., 2008], carbodiimide [Mourya et al., 2008], UV [Felinto et al., 2007] and gamma rays [Felinto et al., 2007] can be used to form chitosan hydrogels. However, a drawback of chemical crosslinker is the toxicity of residual covalent crosslinkers [Liu et al., 2007]. Positively charged nature of chitosan enable it to effectively support cell growth and attach proteins [Zonghua et al., 2007]. Chitosan, as a cationic polymer, is able to form polyelectrolyte complexes with various natural and synthetic polymers. The polyelectrolyte complexes form hydrogels which have been employed in a wide variety of applications such in medicine and pharmacy (especially in drug delivery systems) [Ostrowska et al., 2009]. Many modified chitosan hydrogels also have thermosensitive characteristics. For example, in the study of Bhattaraim et al. (2005), an injectable thermogel was prepared by grafting PEG onto the chitosan backbone and studied for drug release in vitro using bovine serum albumin (BSA) as a model protein. The resulting copolymer formed thermally reversible hydrogels with a lower critical solution temperature of 34°C, and they could also be used as injectable cell-polymer complexes for tissue engineering applications [Bhattaraim et al., 2005]

1.3.2.3 Alginate

Alginate (salt of alginic acid) (Alg) is as a linear, polyanionic polysaccharide that is extracted from brown seaweed and bacteria [West et al., 2007]. It is actually a family of linear copolymers composed of (1-4)-linked β-D-mannuronate (M) and α-L-guluronate (G) residues covalently linked together in different sequences or

blocks (Figure 6). Different ratios of G and M blocks are present in alginate structures due to the large variety of alginate sources. The ratio of these units determines the flexibility of the gels. For example, more flexible gels have a higher M whereas higher G content results in stronger gels [Amsden et al., 1999]. The physical properties and the affinity of the alginates for divalent metal ions are modified by changing the fraction of mannuronic (M) and guluronic (G) residues [Draget et al., 2006]. As seen in Figure 6, alginate gels may be formed via ionic bridges between divalent cations and guluronic acid blocks [Draget et al., 2000]. Many studies argue that steric arrangement of the active groups in the mannuronic and guluronic groups is responsible for this selectivity. [Kohn et al. 1968; Draget et al. 2006]

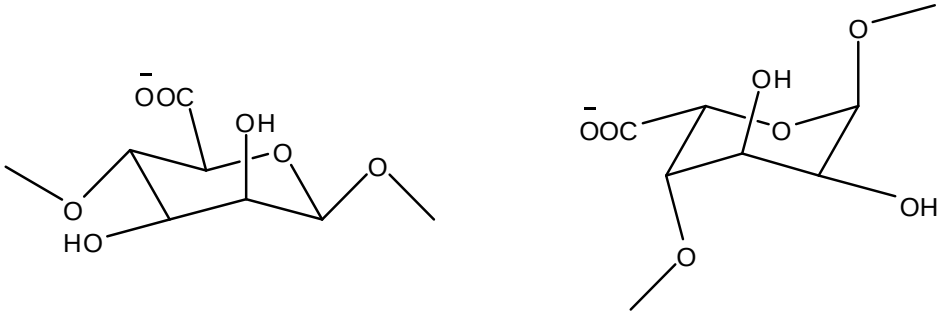

(1→4) β-D-mannuronate (M) α-L-guluronate (G)

Figure 6 The chemical structures of β-D-mannuronic acid and α-L-guluronic acid units of alginate.

Alginate gels have been widely used in enzyme entrapment [Cosnier et al., 2006], wound dressings (especially in combination with gelatin) [Choi et al. 1999; Chiu et al., 2008], stabilizer or gelling agents [Aliste et al., 2000], drug delivery vehicles [Tønnesen et al., 2002], cell transplantation systems [Woźniak et al., 2002] and as injectable delivery vehicle of cells [Kuo et al., 2001]. Moreover, scaffolds for cartilage repair [Almqvist et al., 2009], artificial nerve conduits [Pfister et al.,

2008] and bone filling agents [Alsberg et al., 2001] are some successful examples of alginate hydrogels in tissue engineering.

Alginates can be extensively crosslinked by many crosslinking agents such as glutaraldehyde [Kulkarni et al., 2000], carbodiimides [Chiu et al., 2008] and divalent cations (i.e., Ca^{2+}, Ba^{+2}, Zn^{+2}) [Haug et al., 1965; Nunamaker et al., 2007].

Among these crosslinkers, the most popular crosslinking agents are the divalent cations. In the crosslinking process of alginate, calcium ions interact with the carboxyl groups of the G blocks of two neighboring alginate chains forming egg-box orientation [Nunamaker et al., 2007]. Generally, two crosslinking methods have been proposed and used to fabricate alginate hydrogels, namely, diffusion gelling and in situ gelling. In diffusion gelling, crosslinker diffuses through the liquid alginate boundary while in situ gelling, the crosslinker is mixed with alginate to create a homogeneous mixture (Figure 7). For instance, $CaCl_2$ is an attractive crosslinker used for diffusion gelling of alginate whereas $CaCO_3$ and $CaSO_4$ are the ones that cause in situ gelling through the release of calcium ions for alginate hydrogel formation [Nunamaker et al., 2007].

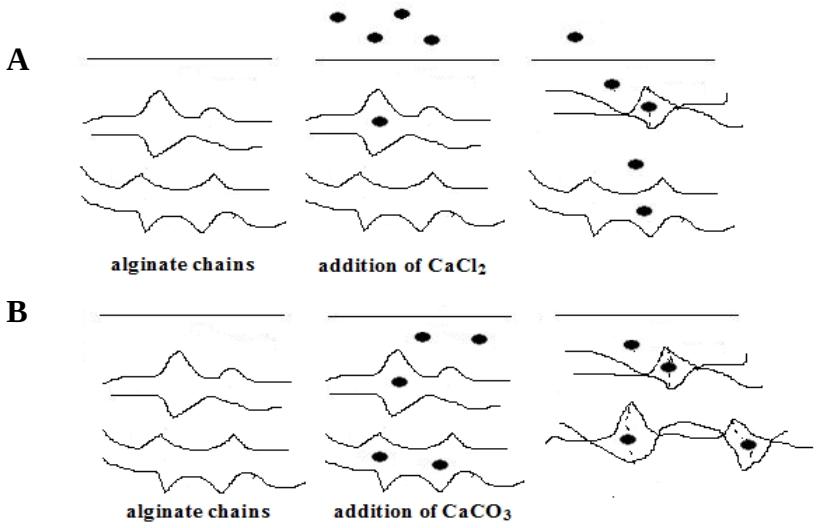

Figure 7 Structure of crosslinked alginate chains in the presence of crosslinker on the egg-box model (A) Diffusion gelling (crosslinker, $CaCl_2$) (B) In-situ gelling (crosslinker, $CaCO_3$).

Although alginate gels have a net negative charge which prevents protein adsorption and reduces cell adhesion, bioactive molecules such as arginine-glycine-aspartic acid (RGD) and fibronectin can be immobilized within the hydrogel to improve the cell adhesion [Park et al., 2004; Novikova et al., 2006].

1.4 Cell Migration Process

Cell motility is quite crucial in tissue engineering applications. Cell migration is regulated by complex, biophysical mechanisms that are influenced by both the chemistry of the extracellular matrix and the surrounding of extracellular environment. While cell migration on 2D surfaces is governed by a balance between counteracting tractile and adhesion forces, many critical biochemical and biophysical parameters should be taken into consideration in order to evaluate cell migration in 3D matrices. ECM significantly influences 3D cell migration by providing microstructural and mechanical support. For this reason, it is important to understand the interplay between the properties of the ECM substitute (3D scaffolds) and the cell migration process. For instance, recent studies show that tailoring three-dimensional scaffolds affects cell migration and its related cellular functions [Mandal et al., 2009; Dutta et al., 2009]. Moreover, numerous studies showed that hydrogels, especially natural based ones, are regarded as cell interactive scaffolds which enhance cell migration [Dutta et al., 2009].

Cell motility starts with the formation of spatial asymmetry of a cell body in order to make the cell body translocate. Migrating cells have highly polarized morphology with complex regulatory pathways. Figure 8 shows the adhesion and motility of the cells. Migration process involves four main steps: polarization of the cell and extension of protrusions in the direction of migration, stabilization of protrusions by adhesion to the ECM, forward movement by contraction and cell detachment at the rear. The physical process of cell movement begins with the retrograde flux of polymerized actin and the cyclical flux of membrane from the rear to the front of the cell. During the migration, first protrusion of lamellae occurs,

then the attachment to the surface takes place, leading to receptor proteins (such as integrins) bind to components of the extracellular matrix (ECM) in order to prevent membrane retraction. The final stage begins with the cell movement involving the disruption or severing of matrix attachments at the rear of the cell and retraction of the trailing edge of the cell. Finally, detachment, or release of adhesion, at the rear of the cell must occur, with retraction of the cell body [Lauffenburger et al., 1996; Ridley et al., 2003]. The migrating cells in 3D, additionally involve proteolytic (most commonly) and nonproteolytic (e.g., in leukocytes) strategies.

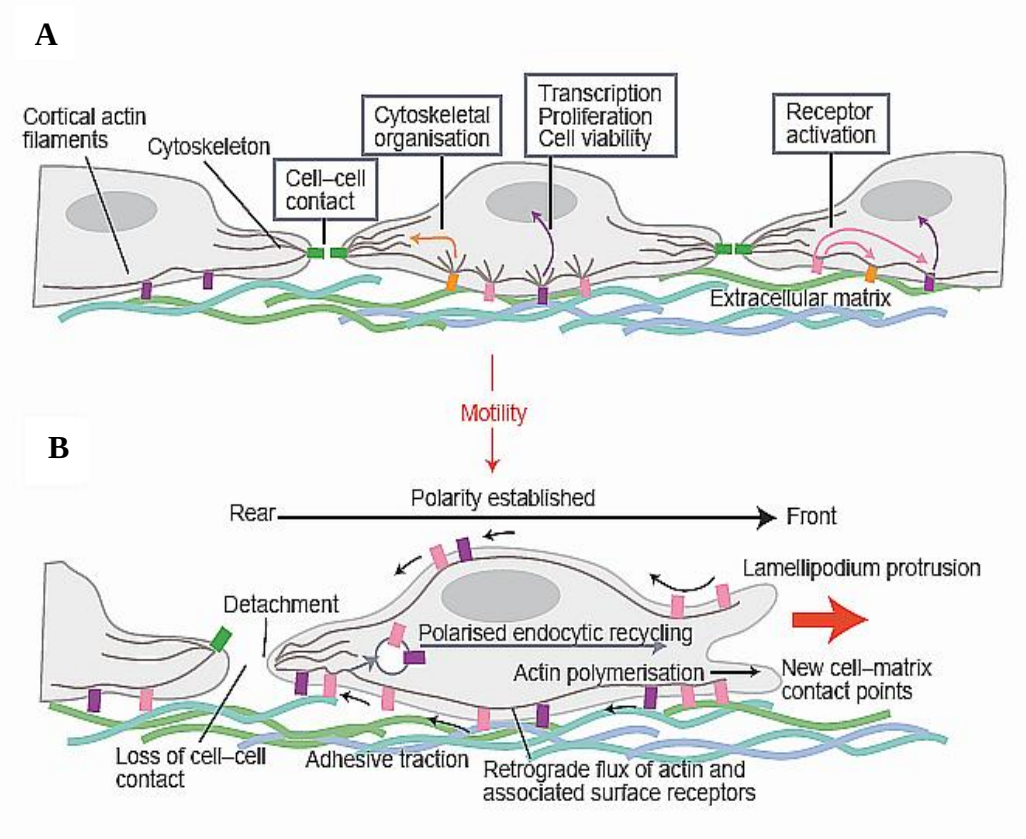

Figure 8 Shematic representation of A) Cell adhesion, B) Cell migration, (Expert Reviews in Molecular Medicine © 1999 Cambridge University Press).

Finally, both cell migration process and ECM scaffold play an extremely important role in tissue morphogenesis and regulation of the development of engineered tissue. Thus, the parameters affecting cell migration should be particularly taken into consideration.

1.5 The Parameters Affecting Cell Migration

Many studies in vivo and in vitro revealed that scaffold matrix geometries and microarchitecture considerably influence the cell migration behavior which is a quite critical requirement for the development of large, porous materials for tissue engineering applications. However, it is still unknown how specific parameters of an ECM substitutes influence cell migration. The following sections will be discussing these parameters.

1.5.1 Porosity

Scaffolds should enable the cells to invade it, proliferate and secrete their own extracellular matrix during formation of a complete and natural tissue. During this process, porosity and pore size of hydrogel scaffolds are considerably critical factors since hydrogels have adjustable pore sizes and their holding large amounts of water enable the transport (diffusion) of gases, nutrients, cells and waste within them. The macroporous structure of hydrogels enables the fast absorption of water by capillary action. This makes the diffusion of soluble substances (e.g. nutrients for cell viability, cellular wastes, etc.) into the center of hydrogel easier. Many studies showed that optimum pore size of macropores of hydrogel scaffolds for cell and tissue penetration should be in the range of 50 nm and 300 μm [Woerly, 2000; Levesque et al., 2005; Chen et al., 2007]. Furthermore, as determined in those same studies, smaller pores, (up to 50 nm) contribute to solute diffusion into the hydrogel. The study focused on the effect of pore size and Young's modulus of negatively charged collagen scaffolds on the migratory behavior of mouse fibroblasts showed

that cell motility was decreased in 3D hydrogel scaffolds as both the pore size (from 50 μm to 160 μm) and elastic moduli (from 206 ± 36 Pa to 1480 ± 210) of the scaffold were increased [Harley et al., 2008]. In the same study, an interesting phenomenon, strut junction (the junction of the interconnected pores) was introduced and it was proposed that increased strut junction density may accelerate ingrowth of cells into the scaffold, regardless of the pore size.

Modification of porosity in hydrogels has therefore been considered as an important process in many ways [Pourjavadi et al., 2010]. Porous hydrogel structures can be obtained by using several methods. The phase separation technique [Studenovska et al., 2008], the use of water soluble porogens [Carenza et al., 1994] and the foaming technique [Ma et al., 2008] are three common widely used methods for having porous hydrogels.

1.5.2 Interconnectivity

Interconnectivity is quite an important parameter that widely influences biological properties of porous scaffolds. Many recent studies have been aiming to enhance pore interconnectivity for tissue engineering applications [Aydin et al., 2009; Annabi et al., 2010]. For example, open, interconnected porous networks enhance the diffusion rate of nutrients and waste materials, leading to preservation viability and the motility of the cells and thus tissue regeneration [Whang et al., 1995].

While demonstrating pore architecture and morphology of hydrogels, it is hard to have complete information about interconnectivity. Scanning electron microscopy (SEM) and mercury (Hg) or helium (He) intrusion porosimetry have commonly been used for determining porosity and pore morphology. SEM provides the image of pore morphology and it is limited to two dimensional (2D) measurements allowing us to observe only a small fraction of a sample, thus it may be difficult to distinguish pores from interconnections. On the other hand, Hg

intrusion porosimetry provides information about the porosity and pore size distribution, but it cannot discriminate connections between pores based on their diameters. Recently, in many studies, 3D micro computed tomography (μ-CT) was used and appears to be as the best method for determining the interconnectivity of the pores (Figure 9) [Aydin et al., 2009; Kim et al., 2009].

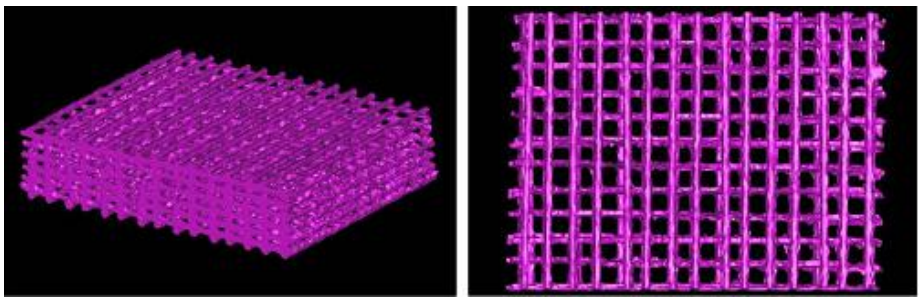

Figure 9 Micro-CT images of a copolymer of PEG, PCL and PLA (Ho et.al, 2006).

1.5.3 Hydrophilicity

Hydrophilicity is especially important for the surface since it comes in contact with the biological environment and determines the compatibility with the environment. Hydrophilicity is a critical factor at the beginning of cell adhesion, then cell proliferation and cell motility. When the surface is moderately hydrophilic (wettable), it can be considered as a quite good support for cell interaction. On the other hand, superhydrophilic or superhydrophobic surfaces do not promote bioadhesion [Marmur et al., 2006]. Surface hydrophilicity can be quantified through measurement of water contact angle and surface free energy (SFE).

Contact angle (θ) is a quantitative value obtained from an equilibrium position between solid-liquid–vapor phases as shown in Figure 10, or it is simply the angle between the vectors of γ_{sl} and γ_{lv}. In this figure, γ_{sl} is the interfacial tension between solid and liquid phases, γ_{lv} is the interfacial tension between liquid and vapor phases and γ_{sv} is the interfacial tension between solid and vapor phases. If

the surface has low energy, γ_{sv} can be defined as $\gamma_{s,}$ and γ_{lv} can be defined as γ_l [Cantin et al., 2005]. So, the relation between the contact angle and the intermolecular forces of the surface can be written as Young's equation:

$$\gamma_{sv} - \gamma_{sl} = \gamma_{lv} \cos \theta$$

Contact angles vary between 0 and 180 degrees. When the surface is entirely wetted by the liquid, contact angle zero is obtained and this indicates that the surface is highly compatible with the liquid and if the liquid is water, it is highly hydrophilic. When the contact angle is above 90°C it is called "non wetting". Any angle between 0°C and 90°C is wetting.

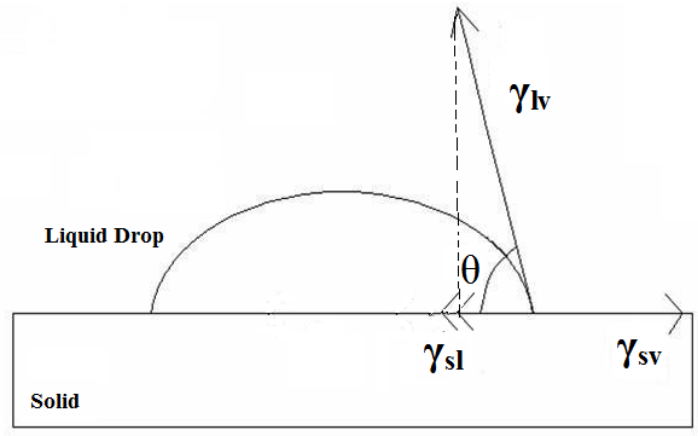

Figure 10 SFE components at equilibrium and the contact angle (**θ**)

Molecules at the surface and in the bulk of a material are exposed to different amounts of forces which are due to the interactions between the neighboring molecules. The molecules in the bulk have no net force acting on them while the ones at the surface encounter a net force inwards as shown in Figure 11. This phenomenon results in a tension or free energy which is called 'Surface Tension' or 'Surface Free Energy' (SFE). In order to break this interaction, at least an equal force should be applied in the opposite direction. For tissue engineering

applications, it is important to have knowledge of the energy or reactivity of surfaces. Present biomaterials in the biomedical field have varying hydrophilicities and SFE values, and there are many studies claiming that the polar and dispersion components of surface free energy affect the adhesion and spreading of cells on polymer surfaces [Harnet et al., 2007; Ozcan et al., 2007; Ozcan et al., 2008].

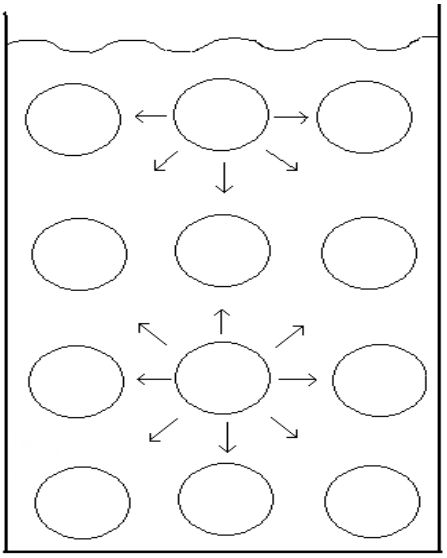

Figure 11 Liquid molecules and interactive forces between them.

SFE is defined as the work required increasing the area of a substance by a unit amount and it has the units of mN/m^2, mJ/m^2, and dynes/cm. For solids, SFE is not a single value but a combination of polar (γ^p) and dispersive (γ^d) components which give information about the polar and nonpolar character of the surface. Their summation gives the total SFE (γ^{tot}). In addition, the polar constituent also has other, acidic (γ^+) and basic (γ^-) components. For solids, all these values can be calculated from the contact angles formed between solid surface and the liquid drops by using various liquids with known component values. SFE components can be calculated by using several approaches such as Harmonic Mean, Geometric Mean and Acid Base [Ozcan et al., 2008] and SFE values can be derived by using following equations.

Harmonic Mean Equation:

$$\gamma_{sl} = \gamma_s + \gamma_{lv} - 4\left(\frac{\gamma_{lv}^d \gamma_s^d}{\gamma_{lv}^d + \gamma_s^d} + \frac{\gamma_{lv}^p \gamma_s^p}{\gamma_{lv}^p + \gamma_s^p}\right)$$

Geometric Mean Equation:

$$\gamma_{sl} = \gamma_s + \gamma_{lv} - 2\left(\sqrt{\gamma_{lv}^p \gamma_s^p} + \sqrt{\gamma_{lv}^d \gamma_s^d}\right)$$

Acid Base Equation is the summation of Lifshitz–van der Waals (γ^{LW}) resulting from the dispersive attractions and polar attractions (γ^{AB}) corresponding to Lewis acid (γ^+) and base (γ^-) components as written in equation 1.4 [Gindl et al., 2001]:

$$(1+\cos\theta)\ \gamma_l = 2\left(\sqrt{\gamma_s^{LW} \gamma_l^{LW}} + \sqrt{\gamma_s^- \gamma_l^+} + \sqrt{\gamma_s^+ \gamma_l^-}\right)$$

In the literature, the results supported that there is an optimum value for both hydrophilicity and surface free energy which promote cell attachment, proliferation and motility [Ozcan et al., 2008; Hasirci et al., 2010].

1.5.4 Charge Effect

The charge density of the scaffold is quite an influential factor on the attachment and migration of cells through the scaffolds. As seen Figure 12, the exterior cell membrane is full of negatively charged membrane components (e.g. proteins, glycolipids, phospholipids) which establish membrane topology. For this reason, the charge distribution is regarded as a strong parameter that affects the cell migration within the scaffold. Many recent studies indicated that charge distribution favored cell ingrowth and cell migration throughout the scaffold [Goda et al., 2009; Janvikul et al., 2007]. In the study of Hermitte et al. (2004), it was shown that strong, negative charges on the material surface provided long range electrostatic

repulsions, and since the living cells are negatively charged, cell adhesion could be prevented [Hermitte et al., 2004]. In a study, neutral PEG polymer, which was copolymerized with positive, negative, or neutral charge densities, was evaluated in terms of cell attachment and it was demonstrated that attachment of fibroblasts on positively charged surfaces was greater than surfaces having negative and neutral charge densities [Schneider et al., 2004].

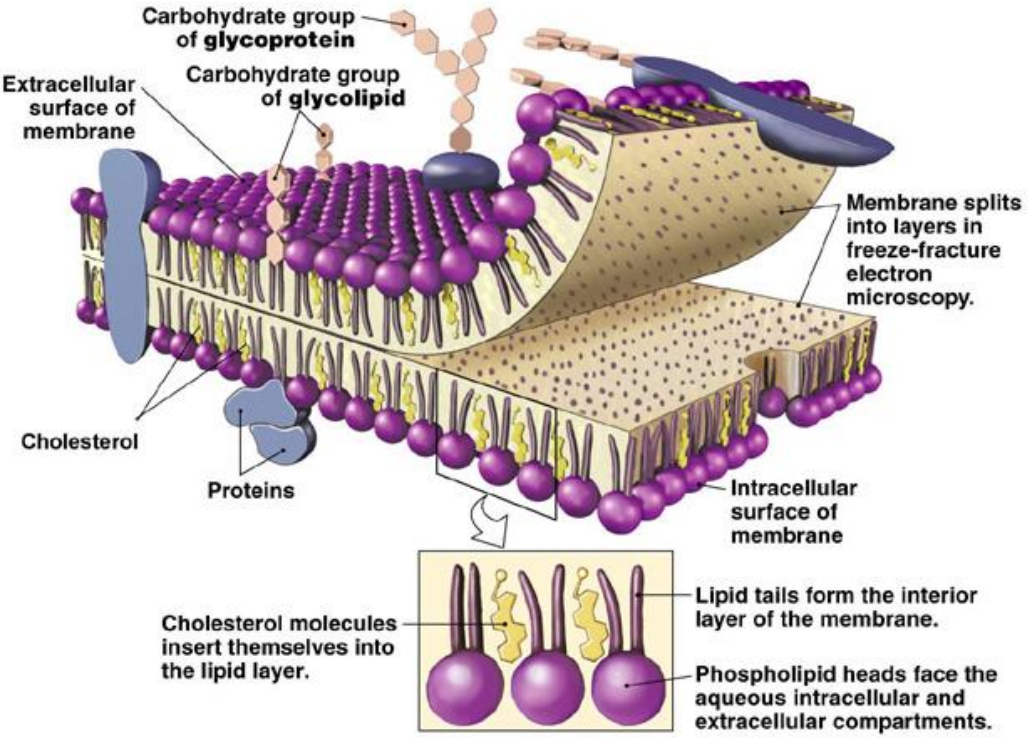

Figure 12 Diagram of the cell membrane, (http://www.colorado.edu/intphys/Class/IPHY3430-200/image/03-4.jpg).

1.6 Aim of the Study

The aim of the present study was to examine effect of different charges on the adhesion, proliferation and migration of cells in the hydrogel scaffolds. For this purpose, semi-interpenetrating network (semi-IPN) structures were prepared by using a natural and neutral biodegradable polymer (agarose) and either positively charged (chitosan) or negatively charged (alginate) polysaccharide, which both are also natural and biodegradable polymers. In the preparation of hydrogels, agarose was thermally crosslinked in the presence of the other polymer which was remained in linear form. Agarose was chosen because it has a high gel forming capacity and neutral structure. Thus, semi-IPN hydrogels with different charges were successfully prepared and their chemical composition, mechanical properties, swelling capacities, and cell affinities towards L929 fibroblast cell line were investigated. The effect of different charges on cell migration within the hydrogel structures was evaluated.

CHAPTER 2

EXPERIMENTAL

2.1 Materials

Agarose (Aga; Sigma Aldrich, Steinheim, Germany), chitosan (Ch; DDA=85%, Sigma Aldrich, Steinheim, Germany), glacial acetic acid (99-100%, J.T. Baker, Netherlands) and alginate (Alg with 61% mannuronic and 39% guluronic acid, M/G ratio of 1.56, medium viscosity, Sigma Aldrich, Steinheim, Germany) were used in the experiments. All liquids used in contact angle and SFE measurements were reagent grade. Formamide ($HCONH_2$) was a product of Merck (Darmstadt, Germany), Diodomethane (CH_2I_2) was a product of Sigma Aldrich (Steinheim, Germany), and dimethyl sulfoxide (C_2H_6OS) was product of Acros (New Jersey, USA). In all the experiments, double distilled water was used. For cell studies, L929 cell line was obtained from Foot-and-Mouth Disease Institute, Ankara, Turkey.

2.2 Methods

2.2.1 Preparation of Hydrogels

Aga, Ch/Aga and Alg/Aga hydrogels were prepared by thermal activation of agarose with the entrapment of chitosan and alginate molecules within the agarose matrix, forming semi-IPN structures. For this purpose, solutions of Aga, Ch, Alg were prepared in PBS solution (10 mM, pH 7.4). To prepare Ch/Aga hydrogels, 2% (w/v) chitosan solution was prepared in 1% acetic acid solution and equal volume

was added dropwise to the same volume of agarose solution by constant stirring at 80°C for 3 h until a homogeneous solution was obtained. To obtain Alg/Aga hydrogels, 2% alginate (w/v) was added dropwise to agarose 2% (w/v) solution by constant stirring at 80°C for 3 h until a homogeneous solution was obtained (Figure 13). Semi-IPNs were prepared by using equal volumes of solutions (at 1:1 volume ratio).

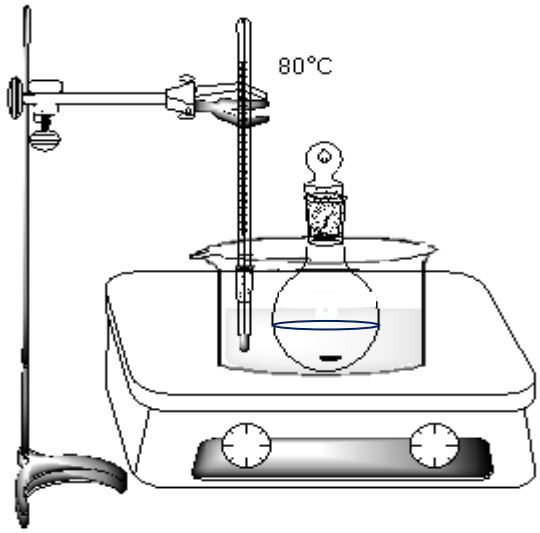

Figure 13 Scheme of hydrogel preparation system.

After 3 hours of stirring, hydrogels were poured into petri dishes. They were allowed to cool to 4°C, then all hydrogels were cut in cylindrical shapes (d = 8 mm, ℓ = 10 mm) with a puncher as seen in Figure 14.

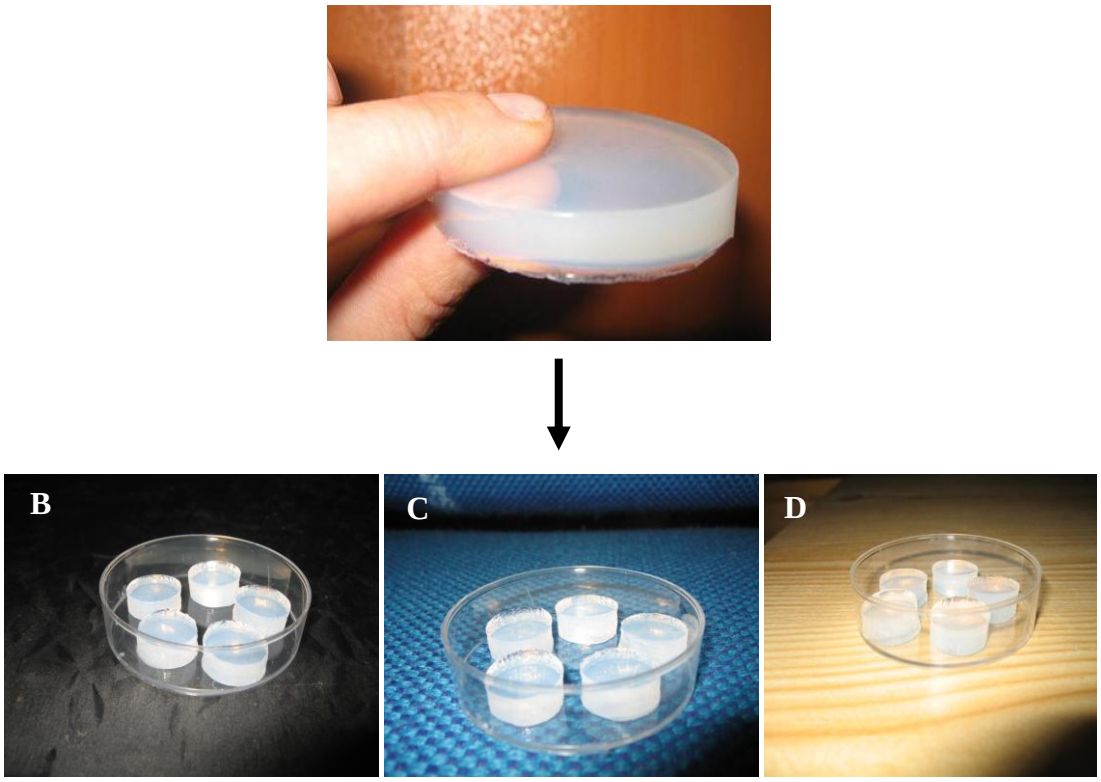

Figure 14 Photographs of hydrogels (A) Before cutting in cylindrical shapes (B) Aga, (C) Ch/Aga, (D) Alg/Aga.

Ch/Aga hydrogels were left in NaOH solution (1 M) for 5 h in order to neutralize the acidic acid and washed with distilled water to remove all the excess NaOH until neutral pH was obtained. For surface free energy (SFE) and contact angle measurements, the similarly prepared polymer solutions of Aga, Ch/Aga, Alg/Aga were cast on microscope slides, dried in an oven for about three to five days at room temperature, then vacuum dried.

2.2.2 Characterization of Hydrogels

2.2.2.1 Fourier Transform Infrared-Attenuated Total Reflectance (FTIR-ATR) Analysis

Chemical compositions of hydrogels were determined by FTIR (FT-IR, SpectrumGX, PerkinElmer, Inc., USA). KBr pellets were prepared from the powders of the samples obtained from the freeze dried and ground hydrogels.

2.2.2.2 Compression Tests

Compression experiments were performed by Lloyd LRX 5K (Lloyd Inst Co., England). The swollen gels were compressed at a rate of 10 mm/min. The ultimate compressive strength (UCS) for each sample was obtained from the ratio of applied force to area. The load-deformation curve was converted to stress-strain curve, where stress is the load per unit area (F/A as Pa) and strain is deformation per unit length ($\Delta l/l_0$), where 1_0 is the initial length in mm and Δl is the change in the length (in mm). Initial slope of the first straight line in elastic region of the stress-strain curve was used for calculating the elastic modulus (in Pa) calculation. For each hydrogel, compression tests were carried out by using at least 5 different samples and the obtained results were averaged.

2.2.2.3 Thermal Analysis

Thermal properties of the samples were determined by differential scanning calorimetry (DSC 6 Perkin Elmer microcalorimeter, USA) and thermogravimetric analysis (TGA 6 Perkin Elmer thermogravimeter, USA). Completely dried samples (7-9 mg) were placed into aluminum pans and heated from 15°C to 450°C at a rate of 10 °C/min under nitrogen atmosphere. For TGA measurements, completely dried samples (3-4 mg) were heated from 15°C to 400°C at a rate of 10 °C/min under nitrogen atmosphere.

2.2.2.4 SFE Determination and Contact Angle Measurements

Different approaches, namely Geometric Mean, Harmonic mean and Acid–base approaches were used to calculate the SFE for hydrogel films. A goniometer (CAM 200, Finland) was used to determine the contact angles at room temperature. In order to calculate SFE values and evaluate surface hydrophilicity of the prepared polymers, liquid drops (5 μL) of deionized water (DW), diiodomethane (DIM), formamide (FA) and dimethyl sulfoxide (DMSO) were placed on the samples and the contact angles of at least five drops were measured and averaged.

2.2.2.5 Swelling

Maximum amount of water absorbed by the samples was calculated from equation 2.1. For this purpose, the hydrogel discs were vacuum dried for 24 h and were weighed. Then they were immersed in PBS (10 mM, pH 7.4) at 37°C for 24 h. The weight of swollen hydrogels was measured in every ten minutes until equilibrium swelling was achieved. For each sample, three parallel experiments were carried out and averaged.

$$\text{Water absorption (\%)} = (W_s - W_d / W_d) \times 100 \qquad (2.1)$$

where W_s and W_d are the swollen and dry weight of hydrogels, respectively.

2.2.2.6 Scanning Electron Microscopy (SEM)

Morphology and porosity of the freeze-dried hydrogels were investigated by scanning electron microscopy (SEM, JEOL JSM-6400, Japan). Both the surface and cross-sections of the samples were sputter-coated with gold prior to examination.

2.3 In Vitro Studies

2.3.1 Cell Attachment and Proliferation

The affinities of the hydrogels for cell attachment, proliferation and migration of the cells through the structures were studied by using L929 fibroblast cells obtained from Foot-and-Mouth Disease Institute, Ankara, Turkey and were derived from mouse connective tissue. Before cell seeding, the hydrogels were cut in disc shape (diameter 8 mm, height 0.5 mm), were sterilized in 70% ethanol for 5 h at 4°C and then washed 3 times with PBS, placed in a 24 well plate and wetted with culture medium prior to cell addition. Cell suspensions (40 μL, containing 50,000 cells) were seeded onto these hydrogels. The gels were kept for 2 h for the attachment of the cells, then DMEM (1 mL) supplemented with 10% FBS penicillin (100 units/mL) and streptomycin (100 μg/mL) was added to each well and cells were incubated at 37°C in a CO_2 incubator for up to a week. The medium was changed in every other day. MTS cell proliferation assay was carried out in order to determine the number of cells colorimetrically using a 96-well Elisa Plate Reader (Maxline, Molecular Devices, USA) at 490 nm. For this purpose, 1 mL of MTS solution was added to each sample in a 24 well plate and incubated for 3 h at 37ºC in the CO_2 incubator. All experiments were performed in triplicate. The proliferation of the cells was calculated on days 1, 3, 7 and 14. After fixation by paraformaldehyde (PFA, 4%) for 15 min, and washing with PBS (10 mM, pH 7.4), the samples were treated with Triton X-100 (1%, 1 mL) for 5 min to permeabilize the cell membranes. In order to prevent non-specific binding, samples were incubated at 37°C for 30 min in BSA-PBS (1%) solution before staining. After washing with 0.1% BSA in PBS, cells on hydrogels were stained with phalloidin (1 μg /1 mL, 400 μL for each) for visualizing actin filaments of the cells. After several washes with PBS, nuclei of the cells were stained with DAPI (400 μL for each). Then, in order to remove the unbound stains, all samples were washed with PBS. The samples were studied with confocal laser scanning microscope (CLSM) (Leica

TCS SPE, Germany) with a 488 nm laser for phalloidin. Cell morphology of hydrogel structures was also studied.

2.3.2 Analysis of Cell Migration within the Hydrogels

For cell migration observations, all hydrogels were cut vertically into two pieces in order to remove the skin layer which was formed at the top of the hydrogels during cooling. Cross-sections of hydrogels were seeded with L929 fibroblast cells (Figure 15).

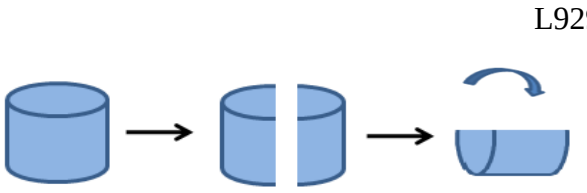

Figure 15 L929 fibroblast cell seeding on cross-section of hydrogels.

At the end of 7 and 14 days of incubation, cell seeded hydrogels were rinsed with PBS (pH 7.4) in order to remove the media and fixed with 4% paraformaldehyde in PBS for 15 min at room temperature. The samples were then treated with 1 mL HCl (1%) for 1 min to permeabilize the cell membranes. After several washes with PBS, the samples were stained with acridine orange (1µg /1 mL, 400 µL for each) for 10 min and studied with the confocal laser scanning microscope (CLSM) with a 532 nm laser in z-stack mode. In order to observe cell migration, images were taken at 2 µm intervals to a depth of 137 µm and visualized in 3D.

CHAPTER 3

RESULTS AND DISCUSSION

3.1 Characterization of Hydrogels

3.1.1 Fourier Transform Infrared Spectroscopy (FTIR)

The FTIR spectra of the polymers and the semi-IPN hydrogels are presented in Figures 16 and 17. The FTIR spectrum of agarose powder showed the characteristic peaks at about 930 cm^{-1} and 1076 cm^{-1} which is assigned to C-C and C-H stretching from alcoholic C-OH groups of agarose and 3,6-anhydrogalactose, respectively (Figure 16). For chitosan, the peaks around 892 cm^{-1} and 1152 cm^{-1} were assigned to the polysaccharide structure and antisymmetric stretching of C-O-C bridge of chitosan. Furthermore, absorption bands at 1402 cm^{-1} for CH_2 bending; at 1633 cm^{-1} for C=O stretching of the N-acetyl group (amide I band) and scissor vibration of amine group; at 1550 cm^{-1} for N-H bending of amide II and scissor vibration of ammonium ions; at 3180 cm^{-1} for stretching of O-H were distinctly shown in the FTIR spectrum of chitosan. For alginate, the characteristic absorption bands around 1130 cm^{-1} and 950 cm^{-1} were C-C stretching and C-O stretching resulted from its polysaccharide structure, respectively (Vieira et al., 2008). Also, the peaks at about 1416 cm^{-1} and 1590 cm^{-1} were due to asymmetric and symmetric stretching of carboxylate salt in alginate Figure 16.

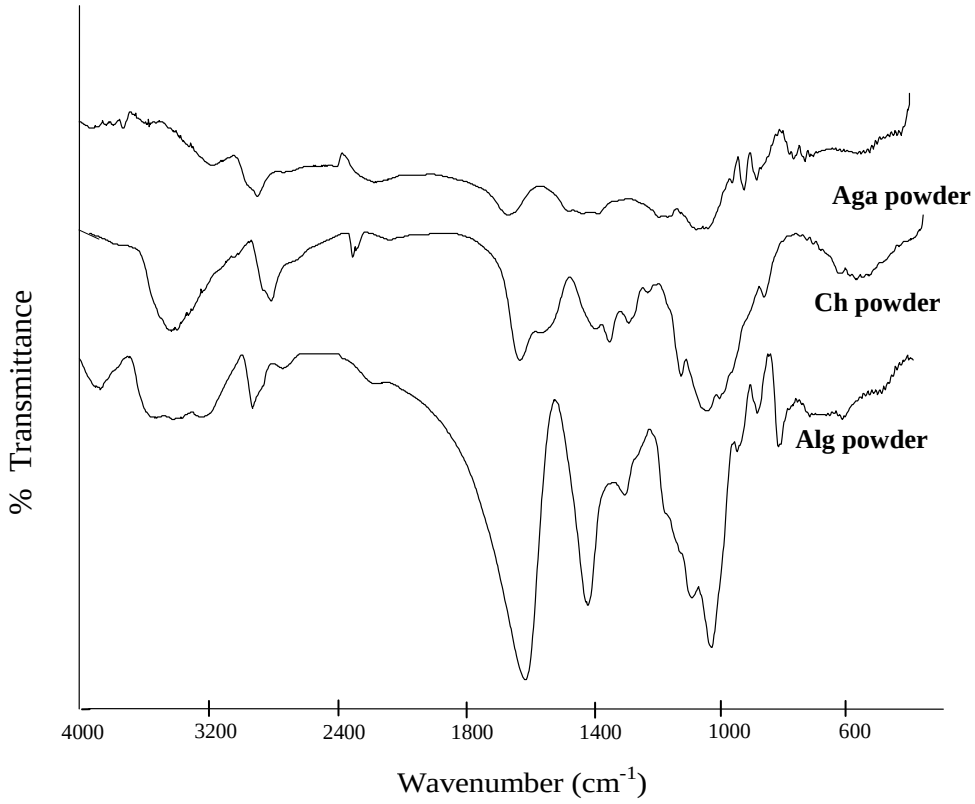

Figure 16 FTIR spectra of Aga, Alg, and Ch powders.

In Figure 17, the broad band at 3300 cm^{-1} which was observed in the spectra of all hydrogels was assigned to the OH stretching of water. The agarose spectrum had peaks near 1074 cm^{-1} due to primary ($-CH_2OH$) and secondary (-CHOH) alcohol groups. In Ch/Aga spectra, the peaks at about 1522 cm^{-1} and 1648 cm^{-1} reveal N-H bending of amide II band (scissor vibration of ammonium ions) and C=O in amide groups (amide I band), respectively. The peak around 1550 cm^{-1} (N-H bending of amide II band) for Ch powder was shifted to 1522 cm^{-1} for Ch/Aga hydrogel as seen Figure 17. This might be because of the interaction between $-NH_3^+$ groups of chitosan and OH^- groups of agarose. The appearance of agarose characteristic peaks (930 cm^{-1} and 1076 cm^{-1}) in all FTIR spectra of semi-IPN hydrogels confirms the presence of chitosan and alginate within the agarose structure.

Although agarose and alginate have very similar chemical structures, the characteristic peak of the Alg/Aga hydrogel was observed at about 1590 cm^{-1} due to C═O antisymmetric stretching of carboxylate salt (–$COONa^{+}$). For Alg/Aga, the peaks at about 1154 cm^{-1}, 1025 cm^{-1}, and 932 cm^{-1} were assigned to C-C stretching, C-O-C stretching, C-O stretching, respectively. The band about 1416 cm^{-1} was due to symmetric stretching peak of the carboxylate salts present in alginate [Vieira, 2008]. The peaks, which were observed all hydrogels spectra, at about 891 cm^{-1}, 930 cm^{-1}, 1076 cm^{-1} were assigned to C-H bending, C-O-C vibration of the 3,6 anhydrogalactose bridge and C-H stretching from alcoholic C-OH groups of agarose and 3,6-anhydrogalactose, respectively.

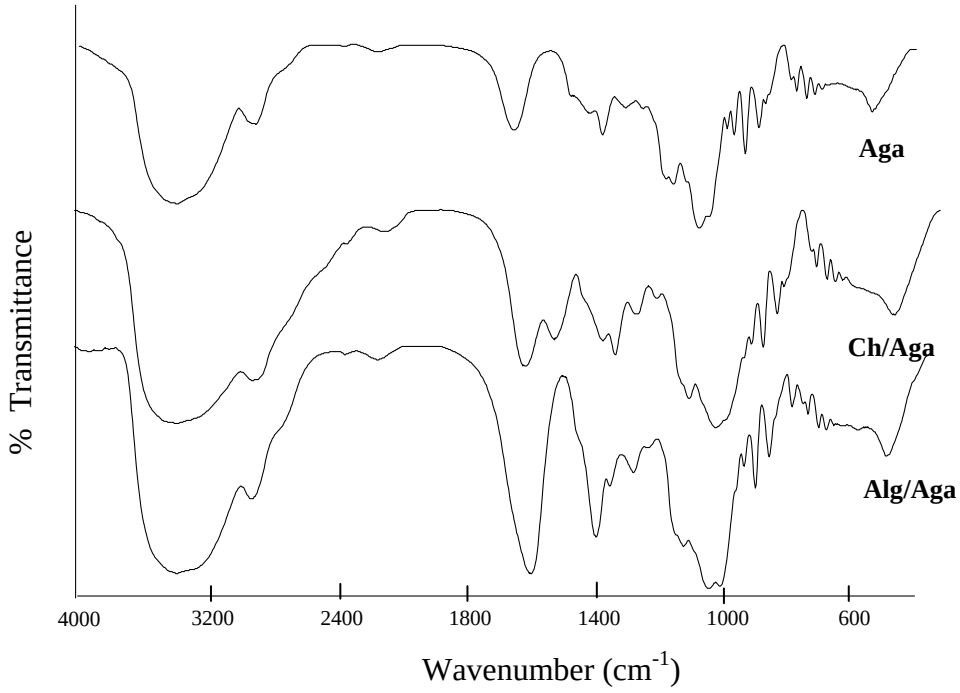

Figure 17 FTIR spectra of Aga, Ch/Aga, Alg/Aga hydrogels.

The spectra of the semi-IPNs revealed the peaks due to the individual biopolymers indicating that the ingredients took them in place in the semi-IPN without detectable interaction between the components.

3.1.2 Compression Tests

Many studies showed that cell migration can be influenced by the mechanical properties of the scaffolds, even in the absence of any soluble chemical stimuli [Pelham et al., 1997; Beningo et al., 2002; Engler et al., 2004]. Cells need to have strong contractile forces for the detachment of adhesions and sense mechanical signals, such as fluid shear, stretching forces and scaffold rigidity. Thus, the feedback mechanism for guiding cell migration can be regulated by both internal and external mechanical forces [Geiger et al., 2001]. Mechanical properties of the hydrogels were obtained by applying compression stress and recording the force applied and change in dimensions. Ultimate compression strength (UCS) and elastic modulus (E) value of the hydrogels are given in Table 2. The agarose hydrogels had the highest elastic modulus value compared to the other structures. During gelling process of agarose coil to helix transition of polymer chains occurs and this conformational change leads to increase in ultimate compression strength and elastic modulus value of agarose.

Within the Ch polymer chains, hydrophobic segments (C-H backbone) are able to create crystal domains [Billmeyer et al., 1984]. Due to these crystalline segments of chitosan, the ultimate compressive strength value was doubled (from 103.11±9.12 Pa to 210.45±5.32 Pa) when Ch was added to agarose. Furthermore, due to the electrostatic interactions between the ammonium (NH_4^+) ions of the chitosan and the hydroxide (OH^-) ions of the agarose, the hydrogen bonding between these molecules was provided to withstand the applied load. On the other hand, almost no significant difference was observed in elastic modulus values of Aga and Ch/Aga hydrogels and both were found around 160 Pa.

The addition of alginate caused a decrease in both ultimate compressive strength and elastic modulus values of agarose hydrogels due to the dynamic transport of water within the alginate polymer chains. The UCS value of agarose decreased from 103.11±9.12 Pa to 91.34± 0.61 Pa upon addition of the negatively charged alginate, most probably due to the electrostatic repulsion between the OH^- ions of the agarose and the $–COO^-$ groups of alginate.

Table 2 UCS and E values of the semi-IPN hydrogels.

Sample	UCS (Pa)	E (Pa)
Aga	103.11 ± 9.12	162.32 ± 7.56
Ch/Aga	210.45 ± 5.32	159.51 ± 3.16
Alg/Aga	91.34 ± 0.61	78.11± 0.92

According to the study of Levental et al. (2007), the elastic moduli (E) of the soft tissues changes between 100 Pa and 100 MPa, thus the mechanical results obtained for the hydrogels were in agreement with the desired values as well as the literature values [Levental et al., 2007].

3.1.3 Thermal Analysis

Due to the thermal changes (e.g. temperature alterations and heat flow rate etc.), important thermal phenomena such as glass transition, denaturation and crystallization temperatures, evaporation temperature of adsorbed water or solvent can be observed during chemical/physical transition. DSC and TGA are two common methods for determining these thermal properties. While DSC measures the rate and degree of heat change as a function of time or temperature, TGA measures changes in mass as function of temperature. In this study, both DSC and TGA were used to study the thermal properties of the prepared hydrogels.

3.1.3.1 Thermogravimetric Analysis (TGA)

The TGA curves of polymers and semi-IPN hydrogels with 10 °C/min heating rate under nitrogen are presented in Figure 18. The first weight loss of agarose occurred at about 80ºC and then the major weight loss step (decomposition) was observed at about 289°C (Figure 18). As explained before, Ch had the highest

thermal stability because of its strong intermolecular interactions. Up to 150°C, the first weight loss corresponds to the loss of adsorbed water of Ch. The second stage of weight loss is due to the degradation of chitosan at 322ºC. The overall decomposition of alginate exhibits two distinct weight loss steps; the first minor weight loss of alginate starts at about 90ºC, the second weight lost occurs above this temperature, degradation was took place up to 270ºC.

Due to the interaction between polysaccharide chains and water, hydrogels released water at different temperatures (Figure 18). The first weight loss step that occur around 100°C might be attributed to the loss of residual water and the major weight loss took place above 250°C for both the polymers and the hydrogels. The decomposition temperature of agarose (270ºC) shifted towards higher values (300ºC) upon Ch addition, which enhances the thermal stability, whereas Alg addition led to the lowest decomposition temperature of 250°C. Thermal stability of Ch/Aga hydrogels may increase because of the electrostatic interactions between the NH_4^+ groups of chitosan and OH^- groups of agarose resulting in more stable structures in these semi- IPNs. On the other hand, for Alg/Aga hydrogels, COO^- groups of alginate and OH^- groups of agarose might repel each other resulting in less stable structures in these semi- IPN structures compared to Aga hydrogels.

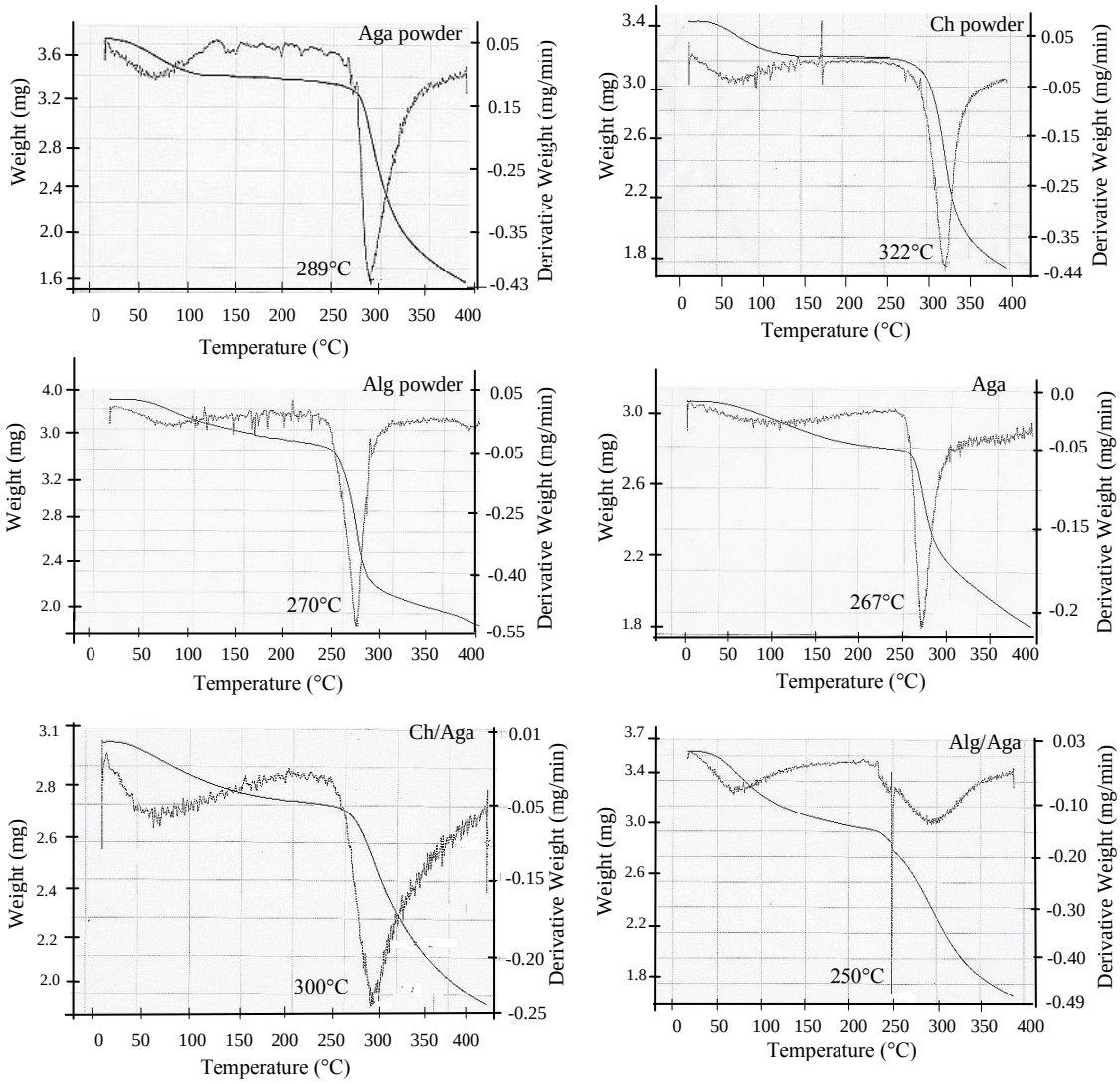

Figure 18 TGA curves of polymers and hydrogels
(heating rate = 10 °C/min, N_2 atmosphere, 20 mL/min).

The decomposition temperatures and water loss of the hydrogels were determined from the DSC graphs (Figure 19) and first derivatives of plotted TGA graphs. The decomposition temperatures and the percentage water loss values of hydrogels presented in Table 3. Both Ch and Ch/Aga hydrogel had the least water evaporation temperatures due to their hydrophobic structure among other structures. The contact angles for Ch and Ch/Aga hydrogels were 78^o and 84°, respectively.

The most significant water loss were detected for Alg/Aga hydrogels which might be probably due to having high swelling capacity compared to other hydrogels (contact angle was 59^{o}).

Table 3 Degradation temperatures of biopolymers and hydrogels obtained with TGA heating rate = 10°C/min, N_2 atmosphere (20 mL/min).

Sample	**Decomposition Temperature (°C)**	**Water Loss**	
		T (°C)	**Net Loss (%)**
Aga powder	289	86.57	16.1
Ch powder	322	67.77	13.2
Alg powder	270	82.56	20.6
Aga	267	83.30	19.3
Ch/Aga	300	62.64	19.4
Alg/Aga	250	82.74	24.8

3.1.3.2 Differential Scanning Calorimetry (DSC)

The DSC curves of polymers and semi-IPN hydrogels at a 10 °C/min heating rate under nitrogen are presented in Figure 19A and 19B, respectively. Since hydrophilic groups of natural polymers usually presents strong interactions with water, the moisture content may influence their thermal properties. The first endothermic broad peak for all samples observed at about 100°C represents the release of water.

The second exothermic peaks with a maximum above 250°C are due to the decomposition of macromolecules where the polymeric chain breaks down. Generally, decomposition that takes place at high temperatures result in the formation of H_2O, CO, CH_4 and, in the case of chitosan, NH_3. The decomposition product of hydrogels around 300°C characterized as a carbonated material.

In Figure 19A, DSC curves of the powder form of the polymers are presented. T_g and melting points are hardly detected for anhydrous polysaccharides because decomposition takes place below the T_g value of these polysaccharides, thus these temperatures could not be recorded in the DSC graphs [Gidley et al., 1993]. Furthermore, rigid backbone structure of agarose, alginate and chitosan resulting from strong inter- and intra- hydrogen bonds prevented the observation of any melting points [Lee et al., 2000]. Sharp exothermic peaks in the DSC thermograms were indicative of decomposition temperatures of the polymers. According to these peaks, agarose started to decompose at about 289ºC. The decomposition temperature of chitosan was observed at about 322ºC whereas Alg had the lowest decomposition temperature at 270°C.

When the DSC graphs of these polymers were compared, a significant water absorption capacity increase was observed as observed in the peak signal ratio (Figure 19B). No melting point was detected for Aga, Ch/Aga and Alg/Aga semi-IPNs. This result was interpreted as the decomposition of these polymers before melting [Mourya et al., 2008]. It is also difficult to observe the glass transition temperature (T_g) of chitosan (150ºC-170ºC) due to its semicrystalline structure. Among the blends, Ch/Aga had the highest degradation temperature (300ºC), which might be a result of the strong intermolecular attractions (hydrogen bonding) between the $–NH_3^+$ of the chitosan backbone and OH^- groups of the agarose as well as formation of some crystalline domains of Ch chains. The decomposition of Alg/Aga has taken place at the lowest temperature (250ºC) compared to those of other hydrogels. Since alginate is a highly negatively charged polyelectrolyte, the electrostatic repulsion between the charged groups of alginate (COO^-) and agarose (OH^-) further contributed to decrease in degradation temperature.

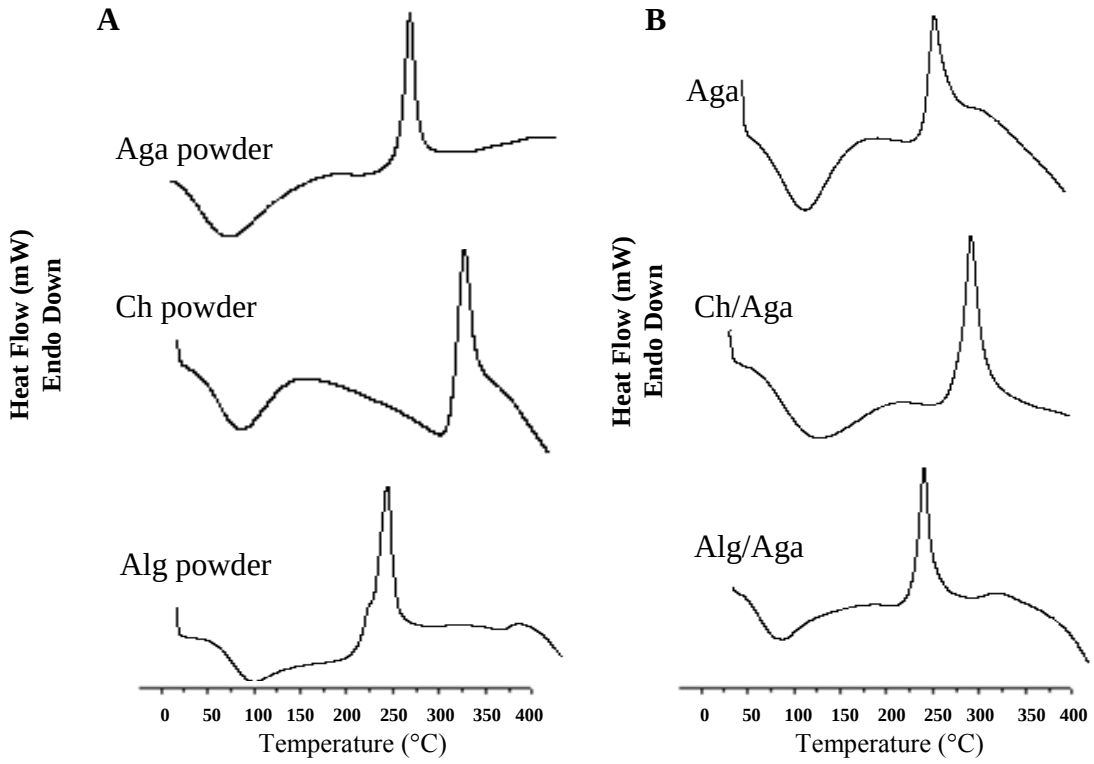

Figure 19 DSC heating curves of polymers (A) and hydrogels (B)
Heating rate = 10°C/min, N_2 atmosphere.

3.1.4 SFE Determination and Contact Angle Measurements

Surface properties of the polymers are quite important for their biocompatibility. Besides knowing the interactions between the polymer molecules, and between the polymer and water molecules and their surface properties, it is necessary to use these properties to have a better understanding of the interfacial interactions of these polymers when in contact with the physiological liquids. Hydrophilicity is an important parameter that is determined by water contact angle measurements and indicated by SFE. SFE measurements were performed by using different liquid couples and triplets to calculate dispersive, polar, acidic and basic components of the SFE. These values were applied to obtain total SFE values by using different approaches, namely Geometric Mean, Harmonic Mean and Acid

Base approaches. SFE and components of SFE values obtained from different approaches (Geometric Mean, Harmonic Mean and Acid Base) are given in Table 4. As can be seen, some differences in SFE values were detected when the applied method was changed. On the other hand, a significant decrease was observed in the polar components of agarose hydrogel upon semi-IPN formation (Ch/Aga and Alg/Aga hydrogels). According to Harmonic mean approach, total SFE of chitosan was 42.07 mJ/m^2 and polar component was 2.95 mJ/m^2. These values increased to 50.34 mJ/m^2 and 13.36 mJ/m^2 in case of Ch/Aga hydrogels, respectively. With chitosan addition to agarose, total SFE decreased from 67.79 mJ/m^2 to 50.34 mJ/m^2, the polar component decreased from 34.91 mJ/m^2 to 13.36 mJ/m^2 and the dispersive component increased from 32.88 mJ/m^2 to 36.97 mJ/m^2. Similarly, significant decrease was also observed in the polar components of Geometric Mean approach. Polar component value of agarose decreased from 32.84 to 8.5 mJ/m^2 upon chitosan addition and to 13.06 mJ/m^2 upon alginate addition. When it is considered for Aga, the higher value of the polar component than that of dispersive component means that the surface has a polar character. High hydrophilicity of agarose can be explained by the contribution of high number of OH groups on the surface of the agarose in its 2D form because the double helical conformation in its solvated form is prevented [Rees et al., 1977]. Although polar molecules such as carboxyl group (COOH) from alginate and amino group (NH_2) from Ch were introduced to agarose, these molecules cause forming a globular structure with agarose, and polar groups turn towards to the bulk because of charge interaction and create a highly rigid backbone [Wang et al., 2009]. It can be concluded that, attractions between the charged groups cause a decrease in their effectiveness causing a decrease in polar components of SFE. It is noteworthy to mention that contact angle results supported these results.

The Acid Base approach showed that agarose hydrogels had the highest values of the acidic (γ^+) and basic (γ^-) components of the SFE as 1.51 and 7.33 mJ/m^2, respectively. These results are in aggrement with the literature [Wang et al., 2009]. Also, in the literature it is stated that the value of dispersive component of

biological surfaces, such as proteins, cells and carbohydrates cannot be more than 45 mJ/m^2 in their dry state [Oss et al., 1995]. In the study, dispersive components of the hydrogels were found very close to this value (maximum 41.29 mJ/m^2) showing their similarity to the biological surfaces. As a conclusion, the results obtained from all approaches were found to be parallel to each other when only total SFE is considered.

Table 4 SFE results of hydrogels and polymers.

Method	**γ^p (mJ/m^2)**	**γ^d (mJ/m^2)**	**γ^+ (mJ/m^2)**	**γ^- (mJ/m^2)**	**γ^{tot}(mJ/m^2)**
Aga					
Harmonic	34.91	32.88			67.79
Geometric	32.84	29.63			62.47
Acid Base	8.58	39.77	1.51	7.33	49.27
Ch/Aga					
Harmonic	13.36	36.97			50.34
Geometric	8.5	38.48			47.07
Acid Base	4.98	41.29	0.74	3.34	46.28
Alg/Aga					
Harmonic	17.14	35.08			52.16
Geometric	13.06	35.37			48.43
Acid Base	4.28	41.21	0.47	4.49	45.49
Ch					
Harmonic	2.95	37.43			42.07
Geometric	6.95	39.11			45.81
Acid Base	1.68	40.73	0.42	1.97	42.45
Alg					
Harmonic	18.20	30.92			49.12
Geometric	16.86	28.90			45.76
Acid Base	4.92	37.53	0.26	3.45	42.45

Water contact angle values were measured by using films of samples prepared on microscope slides and the obtained results were given in Table 5 and Figure 20. The highest water contact angle (84º) was observed for Ch/Aga blends

whereas the lowest water contact angle (27°) for agarose hydrogels. Since agarose hydrogels were prepared as films (2D) for contact angle measurements, coil to helix transition of agarose chains might be prevented so high number of polar groups of agarose (-OH) were present on the surface of the agarose films. This result supported the SFE values of agarose showing high hydrophilicity of agarose compared to other semi-IPN hydrogels. As seen from the Figure 20, agarose shows the highest hydrophilicity having the minimum contact angle (27°). Introducing both chitosan and alginate polymers caused an increase in the water contact angle values of agarose from 27° to 84° and 59°, respectively. This can be a result of the addition of charged polymer to any polymer cause not only to chain rigidity but also also to crystal domains within the structure [Kaufmann et al., 1998; Wiegel et al., 1999; Barikani et al., 2009]. Thus, introducing both alginate and chitosan polymers caused an increase in the water contact angle value of agarose. Also, it was observed that there was no significant differences between the contact angle values of Alg and Alg/Aga hydrogels indicating strong effects of alginate in these samples.

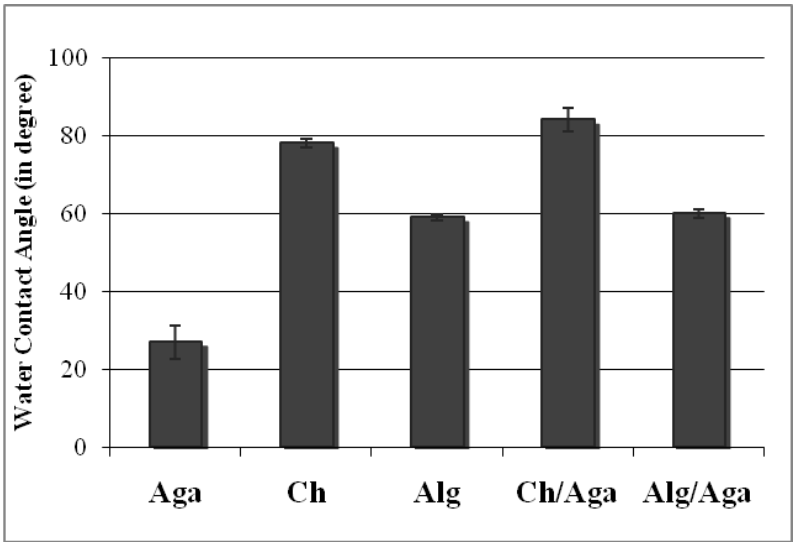

Figure 20 Water contact angles on various hydrogels.

3.1.5 Swelling

The swelling behavior of hydrogel is an important factor for its practical uses. It is a measure of the amount of solvent a material can absorb. In the case when the solvent is water, agarose hydrogel showed quite poor swelling ability (310 %) in comparison to the other semi- IPNs up to 2000 %. This is probably due to its uncharged nature and low polarity also resulting from its helical form transition in its 3D form. This transition also prevented the dynamic transport of water through agarose chains. The presence of the ionic groups of the polymer chains increases swelling because ions are solvated while non-ionic groups do not in the aqueous medium [Mahdavinia et al., 2004]. However, the chain stiffness was increased through the electrostatic interactions between $-NH_3^+$ of chitosan and OH^- ions of agarose, and this leads to a decrease in the swelling ratio of Ch/Aga (580 %) in comparison to Alg/Aga (2036 %) hydrogels where the charges do not neutralize each other. As Alg/Aga has high number of ionizable functional groups like carboxylic acid which caused high water uptake of the polymer, the water absorption value of Alg/Aga was superior compared to other hydrogels.

The percent swelling values of the hydrogels were obtained gravimetrically by weighing the dry and swollen hydrogels in PBS up to 72 hours. The water absorption kinetics of hydrogels were presented in Figure 21. Agarose reaches to its highest swollen state in 5 hours while Alg/Aga and Ch/Aga hydrogels reached to their equilibrium swelling after 3 and 12 hours, respectively. Maximum water absorption (percent swelling) values were calculated as 310 %, 580 % and 2036 % for Aga, Ch/Aga and Alg/Aga, respectively (Table 5).

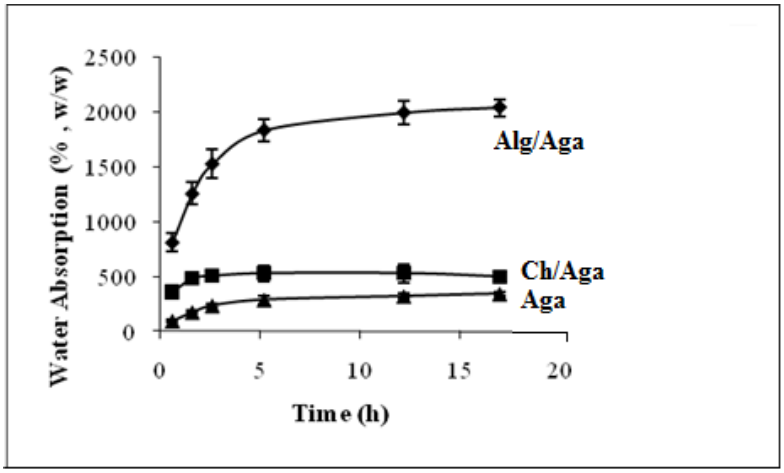

Figure 21 Water absorption of Ag, Ch/Aga and Alg/Aga in PBS, pH 7.4.

Table 5 Water contact angle and water absorption values.

Sample	Contact Angle (θ)	Swelling (%)
Aga	27	310
Ch/Aga	84	580
Alg/Aga	59	2036

3.1.6 Morphology of the Hydrogels

Tissue engineered 3D structures should have a porosity suitable for the in-growth of cells and diffusion of the nutrients. Interconnectivity of the prepared hydrogels was determined by both confocal microscopy (CLSM) and SEM analysis. CLSM images showed that the surface porosities of the hydrogels in their swollen state were quite different from each other.

According to CLSM images taken in the depth of 124 μm, presence of either chitosan or alginate within the agarose structure changed the porosity of the

structures (Figure 22). Aga hydrogels were denser compared to Ch/Aga and Alg/Aga semi-IPNs.

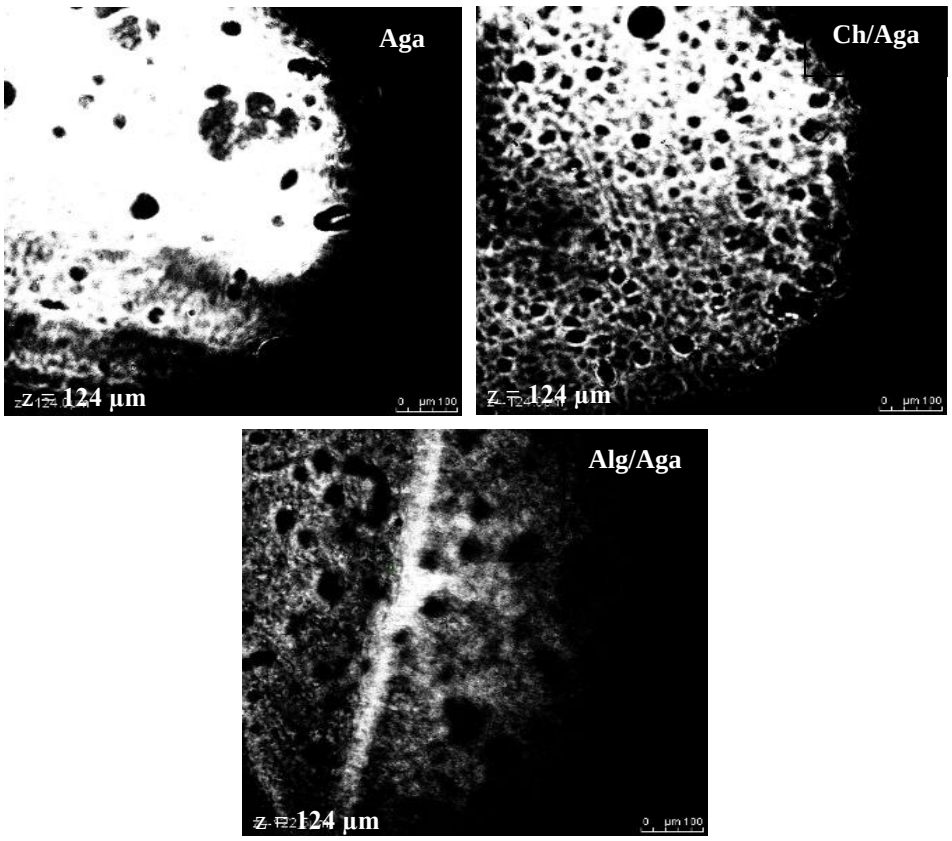

Figure 22 CLSM images of the surface of the hydrogels. White areas represent the polymer-rich phase (scale bar = 100 µm).

According to SEM images, the surfaces of the gels were dense, compact and smooth. On the other hand, large interconnected areas and heterogeneous pore distribution within the structure of lyophilized samples were observed. The appearance of the swollen hydrogel structures observed with CLSM was quite different than the images provided by SEM (Figure 23) for lyophilized samples. It was observed that macroporous hydrogel structures were formed because ice

crystals are formed during the freezing process and by removing these crystals by lyophilization, a more porous appearance is obtained [Zaho et al., 2009].

From SEM images, a skin layer formation was observed on the surface. This result was expected since hydrogels can form skin layers due to dehydration at the surface during gelation [Zhang et al., 2002; Nayak et al., 2003]. With the addition of both chitosan and alginate denser, smaller and interconnected pore structures were obtained. Scanning electron micrographs of lyophilized agarose and other semi-IPN gels revealed open-pore morphology. The pore sizes of the hydrogels calculated from scanning electron micrographs. When cross sections of hydrogels were evaluated, measurements of the pore size values demonstrated that micron pore sized hydrogels were obtained with the addition of Ch or Alg within the agarose.

Pore sizes of the prepared semi-IPN hydrogels were in the range of 100 μm - 1 mm (Aga: 600 μm -1 mm, Ch/Aga: 100 μm - 600 μm and Alg/Aga: 100 μm - 400 μm). According to Schliephake et al. (1991), bone formation occurs if pore size of a material is between 100 μm and 600 μm [Schliephake et al., 1991]. Therefore, pore sizes obtained for Ch/Aga and Alg/Aga hydrogels were in agreement with the desired values for bone tissue engineering.

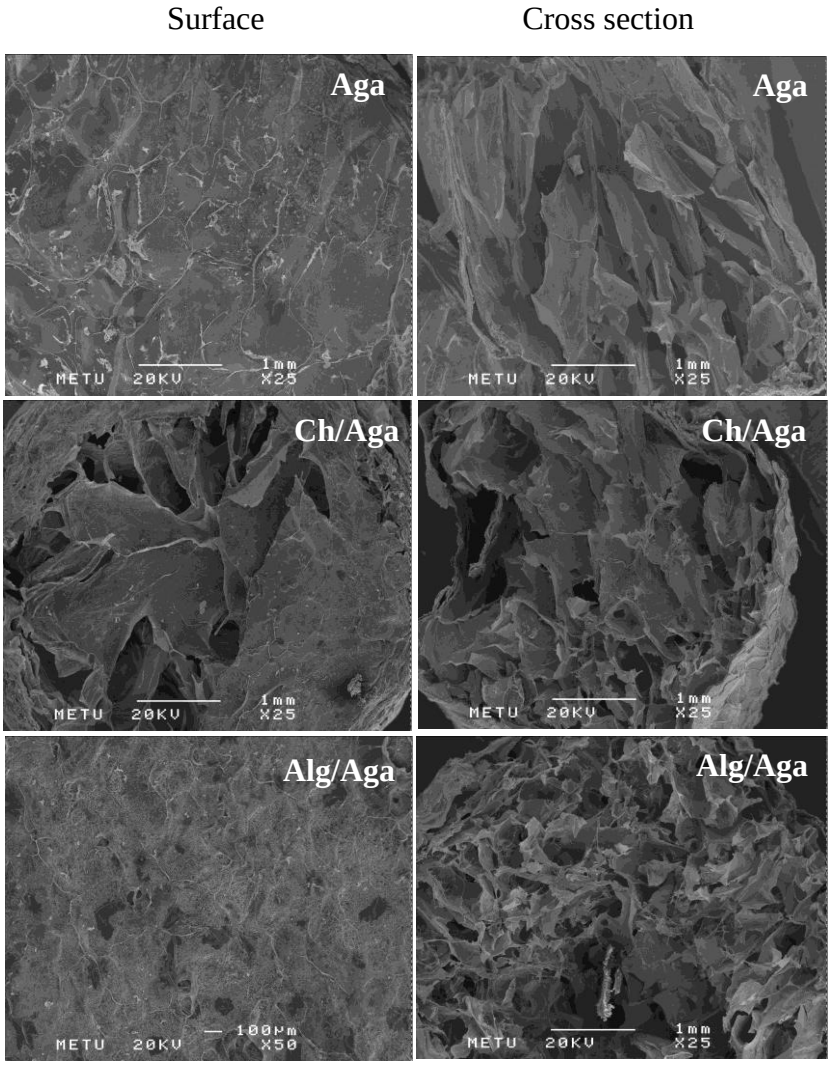

Figure 23 SEM micrographs of the hydrogels.

The hydrogels were immersed in cell culture medium (DMEM) and left for 14 days to check the degradability of the samples. When pore interconnectivity of the hydrogels was examined, it was observed that Ch/Aga hydrogels have still preserved their interconnected pore structure compared to the other hydrogel types (Figure 24).

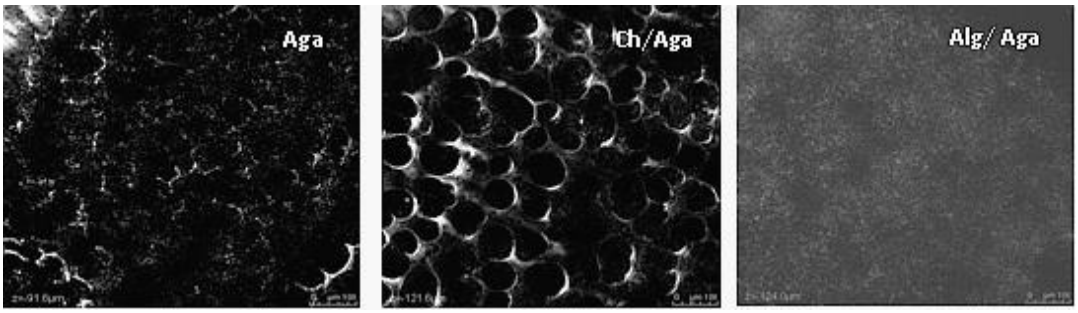

Figure 24 Confocal Microscopy images of the hydrogels left in DMEM Day 14 (scale bar =100 μm).

3.2 In Vitro Studies

3.2.1 Cell Attachment and Proliferation

In vitro response of cells to the hydrogels was evaluated by using the L929 fibroblast cell line which is commonly used in biocompatibility and cell migration studies [Beningo et al., 2001; Buckley et al., 2009; Wiegand et al., 2009]. The cell attachment on hydrogels was evaluated on the first day of cell culture. After fixation of L929 fibroblast cells with 4% PFA, L929 fibroblast cells on the hydrogels were observed on day 1, 7 and 14 by staining nucleus of the cells with DAPI and cytoplasm of the cell with phalloidin. These two stains were chosen in order to overcome the autofluoresce property of chitosan and have clearer cell images. Fluorescence images of these cells on the hydrogels with different charges were obtained. On day 1, L929 fibroblast cells attached and spread very well on Aga and Ch/Aga hydrogels compared to Alg/Aga (Figure 25).

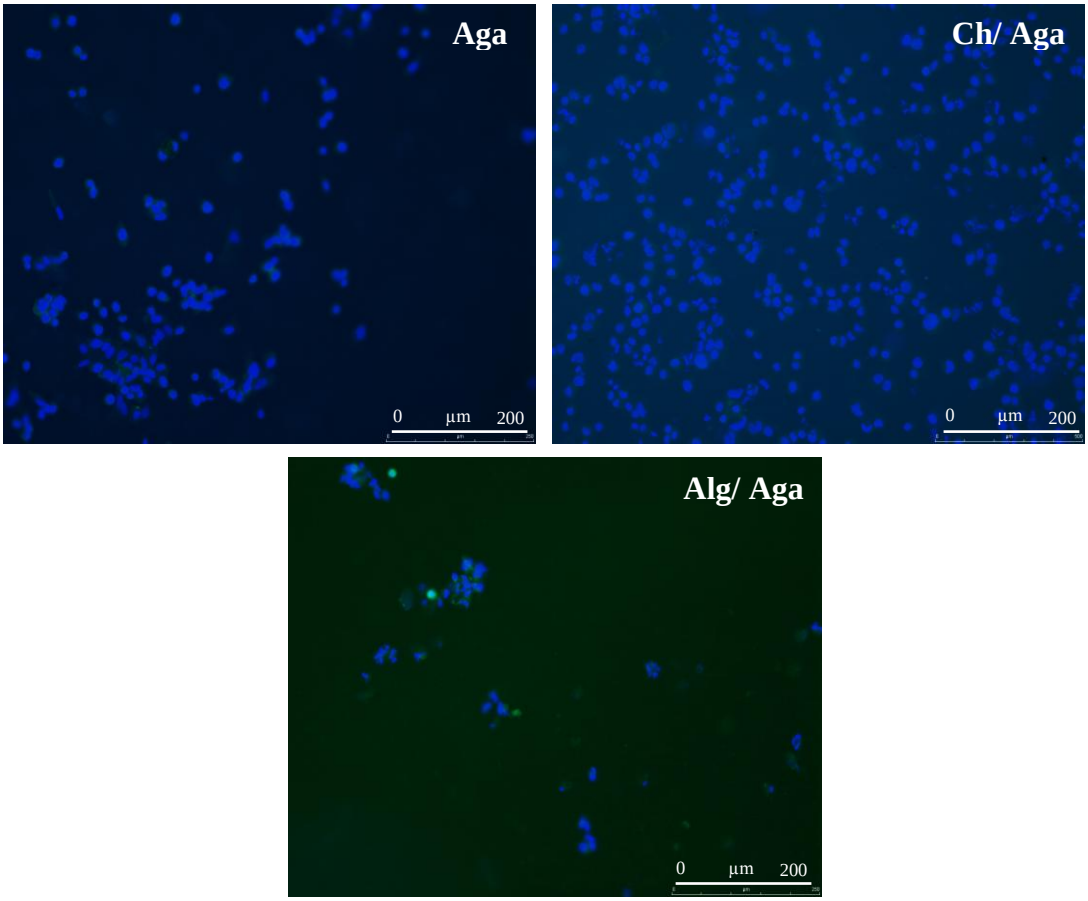

Figure 25 Fluorescence images of DAPI/Phalloidin stained hydrogels on Day 1, (x10).

On day 7, maximum proliferation was observed on Ch/Aga hydrogels (Figure 26). While positively charged chitosan addition within neutral agarose enhanced fibroblast cell proliferation, negatively charged alginate limited cell proliferation which might be because of the electrostatic repulsion between the negatively charged cell membrane and the negatively charged surface of the hydrogel in the early stages of cell adhesion. Also, alginate had the most superior swelling capacity among the hydrogels so the excess water molecules on the alginate surface could prevent cell adhesion.

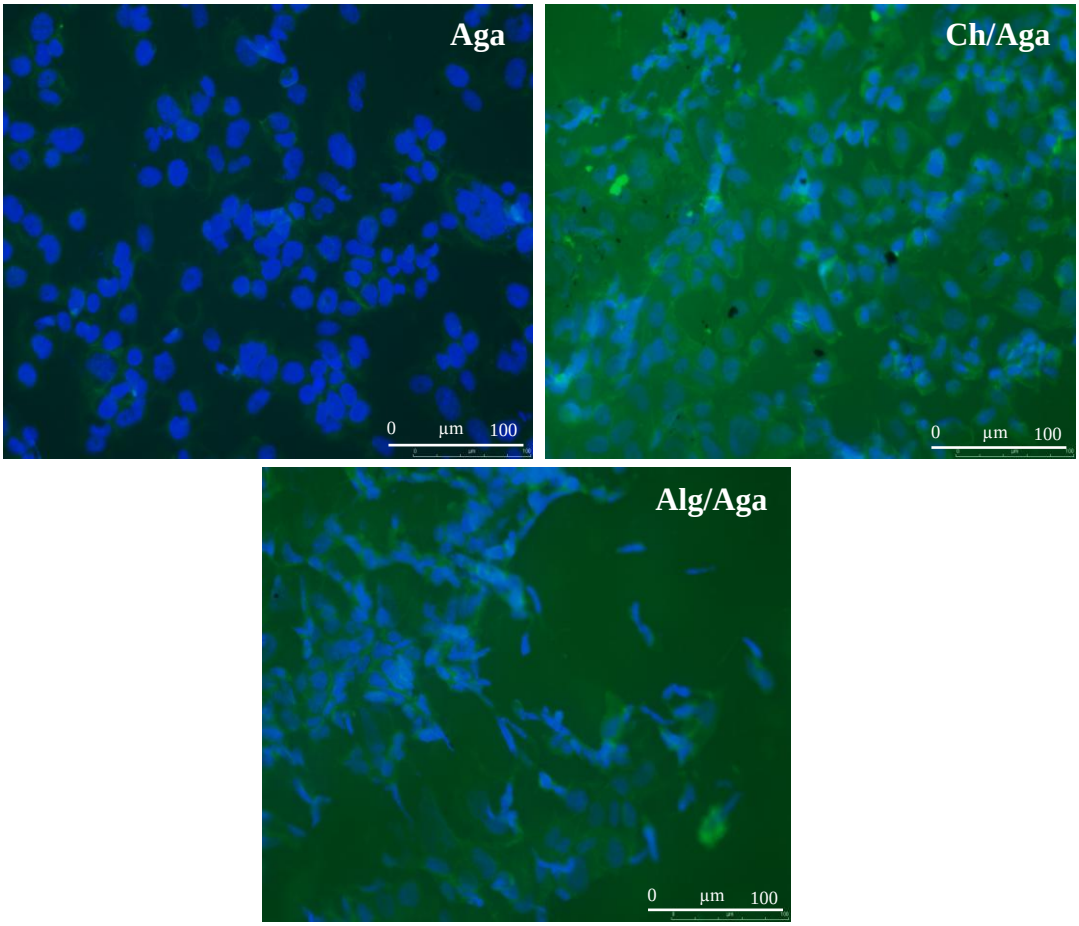

Figure 26 Fluorescence images of DAPI/Phalloidin stained hydrogels on Day 7, (x20).

In order to observe the cell behavior on hydrogels with different charges on day 14, the cells were stained with DAPI/phalloidin (Figure 27). Significantly higher cell was detected on the positively charged Ch/Aga in comparison to neutral Aga and negatively charged Alg/Aga.

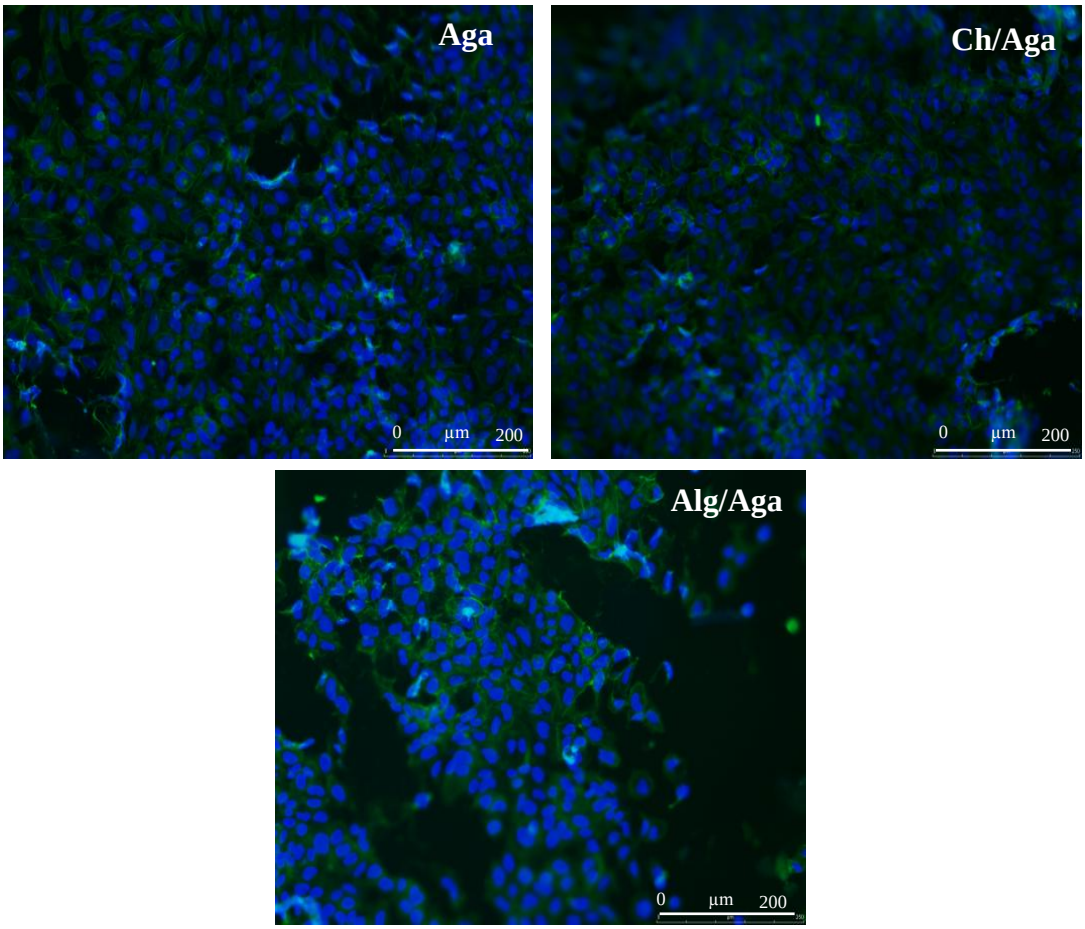

Figure 27 Fluorescence Images of DAPI/Phalloidin stained hydrogels on Day 14, (x10).

In order to quantitatively determine the number of cells on the hydrogels, MTS assay was performed (Figure 28). Many studies have demonstrated that cell adhesion and proliferation are more favorable on reasonably hydrophilic substrates compared to hydrophobic or very hydrophilic ones [Wang, 2007]. However, highest cell proliferation was observed on Ch/Aga although it was stated that Ch/Aga had the most hydrophobic surface (θ =84°) according to contact angle measurements. This probably is because the other hydrogels are either too hydrophilic or too negatively charged or both. Alg/Aga surfaces resulted in lower cell number compared to Ch/Aga. This may be due to dissolution of alginate from the hydrogel causing acidic environment and adversely affects the cell proliferation.

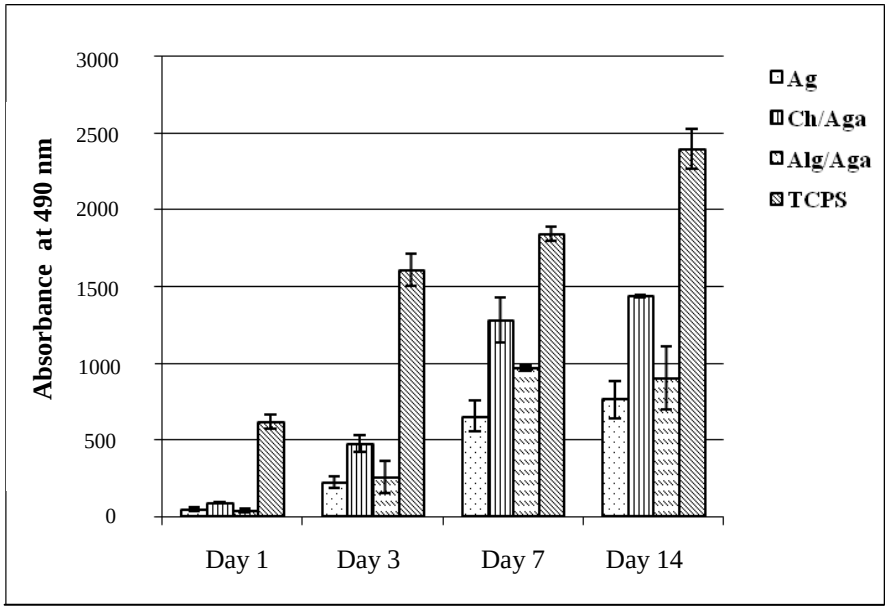

Figure 28 Cell proliferation of L929 cells on hydrogels.

It is not easy to reach a conclusion about a relation between SFE and number of cells attached to the surfaces of hydrogels. Since according the harmonic mean approximation, SFE values were 67.79 mJ/m^2, 50.34 mJ/m^2 and 52.16 mJ/m^2 for Aga, Ch/Aga and Alg/Aga respectively. Although SFE values were quite similar for both semi-IPNs about (50 mJ/m^2), the number of cells attached to the surfaces were significantly different. There are some results reported in the literature showing that the maximum cell attachment occurred on the plasma modified PMMA surfaces which had SFE values of 60 mJ/m^2 [Ozcan et al., 2008]. The contact angle values for the same hydrogels were 27°, 84° and 59°, respectively. Ch/Aga had the most hydrophobic structure with 84° demonstrated the highest cell attachment. Alg/Aga showed 59° and demonstrated lowest cell attachment. The negative result of Alg/Aga could be created by the release of alginic acid into the cell medium.

3.2.2 Analysis of Cell Migration within the Hydrogels

Confocal microscopy was used to evaluate cell penetration through the pores by studying the cell seeded scaffolds. For this reason, the hydrogels were cut in half in order to remove the skin layer formed at the surface during gelation. L929 fibroblast cells were stained with acridine orange and their penetration into the hydrogel scaffolds at day 7 and day 14 at a depth of 137 μm and their 3D arrangement was assessed (Figure 29).

Initially, hydrogel characterization results showed that Aga, Ch/Aga and Alg/Aga hydrogels were significantly different from each other in terms of their porosities, SFE and contact angle values. The depth of cell penetration was different for different hydrogels as seen in Figure 30. For Aga hydrogels, the depth of migration was around 31.4 μm on day 7 and 51.4 μm on day 14 of culturing.The proliferated cells on the surface formed a biofilm, leading to limited cell mobility.

When different charged groups were introduced into the agarose hydrogels, it was observed that the cell penetration behavior was significantly altered. As expected, both highest cell number and the highest penetration were observed for Ch/Aga hydrogels. For these samples, the cells migrated an average distance of 57.1 μm on day 7 and 68.5 μm on day 14. According to the MTS assays (Figure 28) the highest alive cell number was obtained for these samples, and therefore it can be concluded that positively charged environment favored the interaction of the scaffold with cells.

Negatively charged Alg/Aga hydrogels demonstrated the least cell penetration about 28.5 μm on day 7 and 42.8 μm on day 14. The change in the acidity of the medium could cause these results. These findings were in agreement with MTS results.

For all samples, 14 days of incubation caused a biofilm formation and majority of the proliferated cells were accumulated and prevented further cell migration.

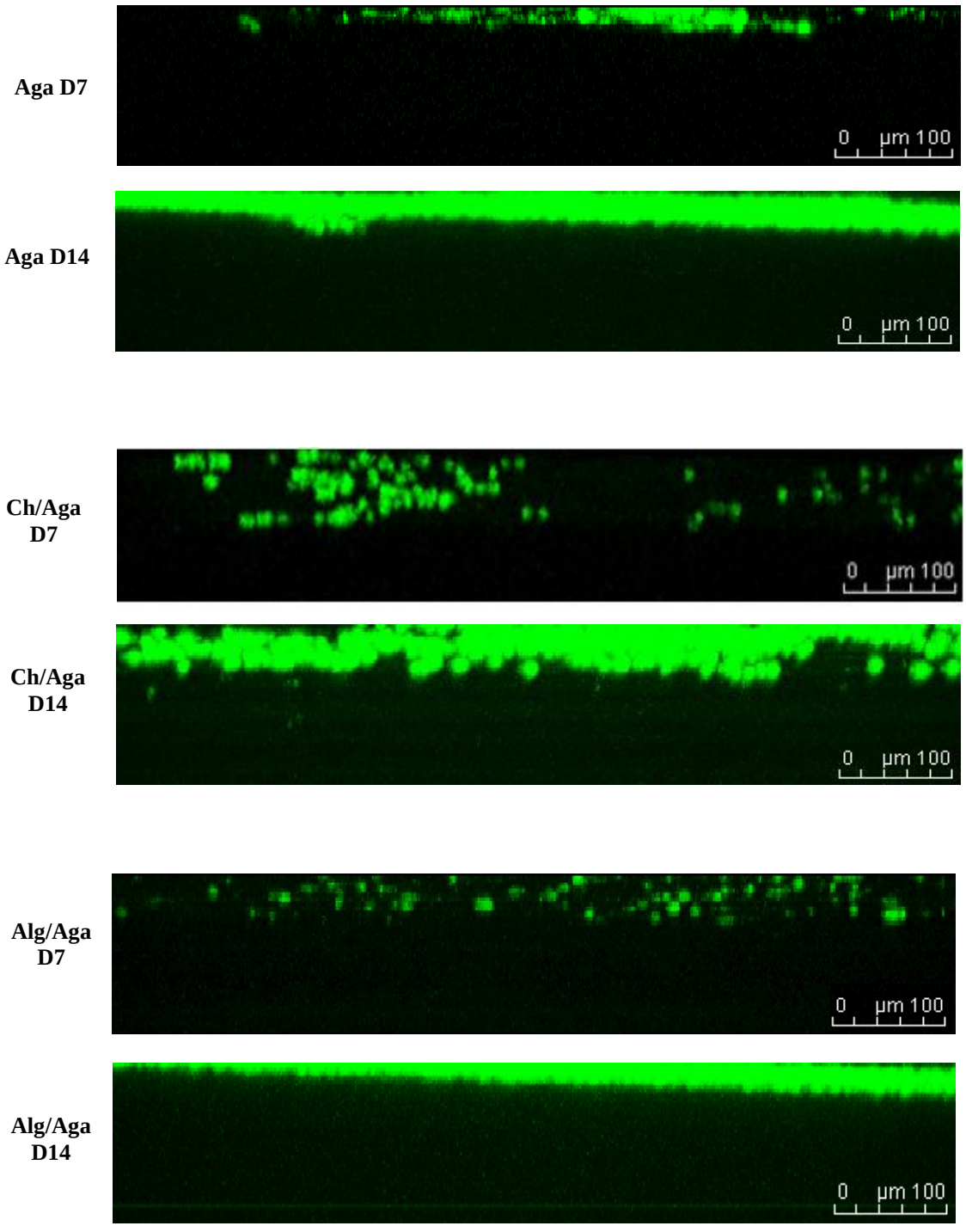

Figure 29 Penetration of the acridine orange stained L929 cells within the hydrogel scaffolds (cross section, z-axis direction).

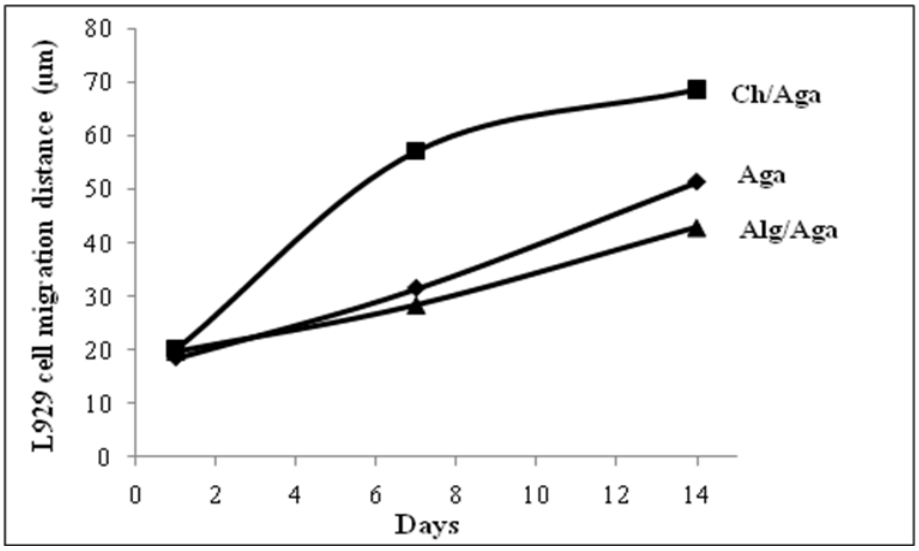

Figure 30 Quantitative analysis of the distance of L929 migration in the hydrogels during two weeks of culture.

So, it can be resulted that according to the confocal examinations, L929 fibroblast cells were able to penetrate and diffuse within the positively charged Ch/Aga hydrogels more easily compared to Aga and Alg/Aga hydrogels.

CHAPTER 4

SUMMARY

Cell attachment and mobility plays quite a crucial role in many biological phenomena. The ultimate aim of tissue engineering methods is to repair functionality of the damaged tissue through the induction and control of cellular behavior within the tissue engineered construct. The goal of this study was to examine the effect of charged microenvironment on cell migration and proliferation with potential application to tissue engineering. Towards this aim agarose based hydrogels with positive, negative and neutral charge were produced. After initial gel characterization, cell proliferation and penetration within these gels were compared. The chemical, thermal and mechanical characterizations of the hydrogels were chiefly performed by FTIR, DSC, TGA and mechanical tester. Water contact angle and SFE measurements were done by using goniometer and swelling capacities were determined gravimetrically. The results obtained in the current study are summarized as follows:

- The FTIR spectra of the semi-IPNs revealed that components of the hydrogels could be detected in the spectra.
- Mechanical analysis results showed that semi-crystalline chitosan addition to agarose enhanced the ultimate compressive strength from 103.11 Pa to 210.45 Pa and decreased the elastic modulus from 162.32 Pa to 159.51 Pa. During gelation, coil to helix transition of polymer chains of agarose led to a stiff gel structure of agarose. On the other hand, the addition of alginate caused a decrease in both ultimate compressive strength and elastic modulus

values of agarose hydrogels due to the dynamic transport of water within the alginate polymer chains.

- In the DSC curves, melting points could not be detected. This is probably due to the decomposition of these polymers prior to melting. Decomposition temperatures of all hydrogels were observed above 250°C. Both DSC and TGA curves confirmed that the addition of chitosan increased the degradation temperature of Aga hydrogel from 267°C to 300°C.
- Hydrophilicity of the semi-IPN hydrogels was evaluated by SFE and contact angle measurements. From the SFE calculations, the polar components of agarose hydrogel were found to have the highest value (8.58 mJ/m^2) among the hydrogels. High hydrophilicity of agarose which was supported by contact angle measurements was due to the high number of polar groups of its solvated form. On the other hand, either chitosan or alginate addition has decreased the surface hydrophilicity because of their charged nature, led to chain rigidity.
- Both chitosan and alginate containing agarose hydrogels resulted in an overall trend toward increasing swelling in equilibrium. A significant increase was observed in water intake of alginate containing hydrogels when compared to other hydrogels. This result indicated that alginate had high number of ionizable functional groups like carboxylic acid which caused high water uptake of the polymer compared to other prepared hydrogels. However, the increase in swelling capacity of the Alg containing hydrogels did not have an effect on hydrophilicity most probably due to the highly charged rigid chain structure in its 2D form.
- SEM analysis demonstrated that hydrogel surfaces were dense, compact and smooth. On the other hand, large interconnected areas and heterogeneous pore distribution within the structure of lyophilized samples were observed.
- L929 cell line was used to examine cell interaction with the hydrogels. Much better cell attachment and proliferation on Ch/Aga semi-IPN's were

observed compared to Aga and Alg/Aga hydrogels in the confocal images of the cells and MTS assay.

- The effect of the charged microenvironment on cell migration and proliferation were assessed by confocal microscopy on day 7 and day 14 with a maximum depth of 137 μm.
- L929 fibroblast cells were able to penetrate and diffuse within the positively charged Ch/Aga hydrogels more easily compared to Aga and Alg/Aga hydrogels.

As a result, Ch/Aga hydrogel scaffolds could be thought as quite a promising candidate for tissue engineering applications. Additional modifications upon the Ch/Aga hydrogel would make possible to control and improve cell migration into these scaffolds. Excitingly, an ‘optimal’ smart scaffold option can be created to direct cell migration in vivo for tissue engineering applications.

REFERENCES

Aliste, A. J., Vieire, F., Del Mastro, N. L., 'Radiation effects on agar, alginates and carrageenan to be used as food additives', Radiation Physics and Chemistry, 57: 305-308, 2000.

Almirall, A., Larrecq, G., Delgado, J.A., Martínez, S., Planell, J.A., Ginebra, M.P., 'Fabrication of low temperature macroporous hydroxyapatite scaffolds by foaming and hydrolysis of an α-TCP paste', Biomaterials, 25: 3671-3680, 2004.

Almqvist, K. F., Dhollander, A. M., Verdonk, P. C. M., Ramses Forsyth, Verdonk, R., Verbruggen, G., 'Treatment of Cartilage Defects in the Knee Using Alginate Beads Containing Human Mature Allogenic Chondrocytes', Journal of Sports Medicine, 37: 1920-1929, 2009.

Amsden B, Turner N. 'Diffusion characteristics of calcium alginate gels', Journal of Biotechnology Bioengineering, 65: 605–610,1999.

Annabi, N., Mithieux, S. M., Weiss, A. S., Dehghan, F., 'Cross-linked open-pore elastic hydrogels based on tropoelastin, elastin and high pressure CO_2', Biomaterials 31: 1655-1665, 2010.

Aydin, H. M., El Haj, A. J., Piskin, E., Yang, Y., 'Improving pore interconnectivity in polymeric scaffolds for tissue engineering', Journal of Tissue Engineering and Regenerative Medicine, 3: 470 – 476, 2009.

Aymard, P., Martin, D.R, Plucknett, K., Foster, T. J., Clark A. H., Norton, I. T., 'Influence of thermal history on the structural and mechanical properties of agarose gels', Biopolymers, 59: 131-44, 2001.

Baidya, K. P., Ramakrishna, S., Rahman, M., Ritchie, A., Huang, Z., 'An Investigation on the Polymer Composite Medical Device – External Fixator', Reinforced Plastics and Composites, 22: 563, 2003.

Barikani, M., Honarkar, H., Barikani, M., 'Synthesis and Characterization of Polyurethane Elastomers Based on Chitosan and Poly(e-caprolactone)', Applied Polymer Science, 112: 3157–3165, 2009.

Basmanav, F. B., Torun Kose, G., Hasirci, V., 'Sequential Growth Factor Delivery From Complexed Microspheres For Bone Tissue Engineering', Biomaterials, 29: 4195-4204, 2008.

Bhattaraim, N., Ramay, H.R., Gunn, J., Matsen, F.A. and Zhang, M.Q., 'PEG-grafted chitosan as an injectable thermosensitive hydrogel for sustained protein release', Journal of Controlled Release, 103: 609–624, 2005.

Beningo, K.A., Lo, C.M., Wang, Y.L., 'Flexible polyacrylamide substrata for the analysis of mechanical interactions at cell-substratum adhesions', Methods Cell Biology, 69: 325–339, 2002.

Berger, J., Reist, M., Mayer, J. M., Felt, O., Gurny, R., 'Structure and interactions in chitosan hydrogels formed by complexation or aggregation for biomedical applications', European Journal of Pharmaceutics and Biopharmaceutics, 57: 35–52, 2004.

Bica, C. I. D., Borsali, R., Geissler, E., Rochas, C. 'Dynamics of Cellulose Whiskers in Agarose Gels. 1. Polarized Dynamic Light Scattering', Macromolecules, 34: 5275–5279, 2001.

Billmeyer, F.W., Textbook of Polymer Science (3rd ed), John Wiley & Sons, New York (1984) (Chapter 12).

Buckley, C. T., Thorpe, S. D., Brien, F. J., Robinson, A. J., Kelly, D. J., 'The effect of concentration, thermal history and cell seeding density on the initial mechanical properties of agarose hydrogels', Mechanical Behavior of Biomedical Materials, 2: 512-521, 2009.

Buckwalter, J.A., 'Musculoskeletal tissues and the musculoskeletal system' in Turek's Orthopaedics Principles and their Applications, Wenstein, S.L., Buckwalter, J.A. eds., Lippincott Company, 2005.

Cantin, S., Bouteau, M., Benhabib, F., Perrot, F., 'Surface free energy evaluation of well-ordered Langmuir–Blodgett surfaces, Comparison of different approaches', Colloids and Surfaces A: Physicochemical and Engineering Aspects, 276: 107-115, 2005.

Carenza, M., Veronese, F.M., 'Entrapment of biomolecules into hydrogels btained by radiation-induced polymerization', Journal of Control Release, 29: 187–193, 1994.

Cao, T., Ho, K.H., Teoh, S.H., 'Scaffold design and in vitro study of osteochondral coculture in a three-dimensional porous polycaprolactone scaffold fabricated by fused deposition modeling', Tissue Engineering, 9: 103-112, 2003.

Chaoliang, C., Kim, S. W., Lee, D. S., 'In situ gelling stimuli-sensitive block copolymer hydrogels for drug delivery', Journal of Controlled Release, 127: 189–207, 2008.

Chen, F.M., Zhao, Y.M., Sun, H.H., Jin, T., Wang, Q.T., Zhou, W., Wu, Z, F., Jin, Y., 'Novel glycidyl methacrylated dextran (Dex-GMA)/gelatin hydrogel scaffolds containing microspheres loaded with bone morphogenetic proteins: Formulation and characteristics', Journal of Controlled Release 118: 65–77, 2007.

Chiu, C.T., Lee, J.S., Chu, C. S., Chang, Y.P., Wang Y.J., 'Development of two alginate-based wound dressings', Journal of Materials Science: Materials in Medicine, 19: 2503–2513, 2008.

Chou, A.I., Akintoye, S.O., Nicoll, S.B., 'Photo-crosslinked alginate hydrogels support enhanced matrix accumulation by nucleus pulposus cells in vivo', Osteoarthritis and Cartilage, 17: 1377-1384, 2009.

Chouhan, R., Bajpai, A.K., 'Real time in vitro studies of doxorubicin release from PHEMA nanoparticles', Nanobiotechnology,7: 5, 2009.

Connor, N.E., Mulliken, J.B., Banks-Schlegel, S., Kehinde, O., Green, H., 'Grafting of burns with cultured epithelium prepared from autologous epidermal cells', Lancet, 82: 75–78, 1981.

Cosnier, S., Christine, M., Chantal, G., Lepellec, A., 'Entrapment of enzyme within organic and inorganic materials for biosensor applications: Comparative study', Materials Science and Engineering, 26: 442–447, 2006.

Costa, R.O.R., Pereira, M. M., Lameiras F. S., Vasconcelos W.L. 'In vitro study of apatite precipitation on poly (2-hydroxyethyl methacrylate)-silica hybrids with controlled surface areas', Key Engineering Materials, 240-242: 195-198, 2003.

Desai, S., Ravi, M., 'Polymers, Composites and Nano Biomaterials: Current and Future Developments', Bio-Materials and Prototyping Applications in Medicine, Springer, 2008.

Djagny, K. B., Wang, Z., Xu, S., 'Gelatin: a valuable protein for food and pharmaceutical industries: review', Critical Reviews in Food Science and Nutrition, 41: 481–492, 2001.

Dodla, M.C., Bellamkonda, R.V., ‘Differences between the effect of anisotropic and isotropic laminin and nerve growth factor presenting scaffolds on nerve regeneration across long peripheral nerve gaps’, Biomaterials, 29: 33-46, 2008.

Dornish, M., Kaplan, D., Skaugrud, O. ‘Standards and guidelines for biopolymers in tissue-engineered medical products’, Annals of the New York Academy of Sciences, 944: 388–97, 2001.

Draget, K. I., Strand, B., Hartmann, M., Valla, S., Smidsrød, O., Skjak Bræk, G., ‘Ionic and acid gel formation of epimerised alginates; the effect of AlgE4’, International Journal of Biological Macromolecules, 27: 117–122, 2000.

Draget, K. I., Skjak-Bræk, G., Stokke, B. T., ‘Similarities and differences between alginic acid gels and ionically crosslinked alginate gels’, Food Hydrocolloids, 20: 170–175, 2006.

Dutta, R. C., Dutta A. K., ‘Cell-interactive 3D-scaffold; advances and applications’, Biotechnology Advances, 27: 334–339, 2009.

Eisenbarth, E., ‘Biomaterials for Tissue Engineering’, Advanced Engineering Materials, 9: 1051-1060, 2007.

Engler, A., Bacakova, L., Newman, C., Hategan, A., Griffin, M., Discher, D., ‘Substrate compliance versus ligand density in cell on gel responses’, Biophysical Journal, 86: 617–628, 2004.

Faxälva, L, Ekblad, T., Liedberg, B., Lindahl, T. L., ‘Blood compatibility of photografted hydrogel coatings’, Acta Biomaterialia, 6: 2599-2608, 2010.

Fee, C.J., Alstine, J. M., V.,‘PEG-proteins: Reaction engineering and separation issues’, Chemical Engineering Science, 61: 924 – 939, 2006.

Felinto, M.C.F.C., Parra, D.F., Silva, C.C., Angeramia, J., Oliveira, M.J.A., Lugão, A.B., 'The swelling behavior of chitosan hydrogels membranes obtained by UV- and γ-radiation', Nuclear Instruments and Methods in Physics Research Section B: Beam Interactions with Materials and Atoms, 265: 418-424, 2007.

Filmon, R., Baslé, M.F., Barbier, A., Chappard, D., 'Poly(2-hydroxy ethyl methacrylate)-alkaline phosphatase: A composite biomaterial allowing in vitro studies of bisphosphonates on the mineralization process', Journal of Biomaterials Science Polymer Ed, 11: 849-868, 2000.

Fuchs, S., Ghanaati, S., Orth, C., Barbeck, M., Kolbe, M., Hofmann, A., Eblenkamp, M., Gomes, M., Reis, R. L., Kirkpatrick, C. J., 'Contribution of outgrowth endothelial cells from human peripheral blood on in vivo vascularization of bone tissue engineered constructs based on starch polycaprolactone scaffolds' Biomaterials, 30: 526-534, 2009.

Geiger, B., Bershadsky, A., 'Assembly and mechanosensory function of focal contacts', Current Opinion in Cell Biology, 13: 584-592, 2001.

Gidley, M. J., Cooke, D., Ward-Smith, S., Low-moisture polysaccharide systems: Thermal and spectroscopy aspects. In J. M. V. Blanshard & P. J. Lillford (Eds.), The glassy state in foods (pp. 303–316). Nottingham: Nottingham Univ. Press, 1993.

Gindl, M., Sinn, G., Gindl, W., Reiterer, A., Tschegg, S., 'A comparison of different methods to calculate the surface free energy of wood using contact angle measurements', Colloids and Surfaces A: Physicochemical and Engineering Aspects, 181: 279–287, 2001.

Goda, T., Goto, Y., Ishihara, K., Cell-penetrating macromolecules: Direct penetration of amphipathic phospholipid polymers across plasma membrane of living cells, Biomaterials, 31: 2380-7, 2009.

Gomes, M.E., Reis, R.L., 'Biodegradable polymers and composites in biomedical applications: from catgut to tissue engineering. Part 2 Systems for temporary replacement and advanced tissue regeneration', International Materials Reviews, 49: 274–285, 2004.

Goycoolea, F.M., Argüelles-Monal, W.M., Lizardi, J. C., Peniche, Heras, A., Galed, G., Díaz, E.I., 'Temperature and pH-sensitive chitosan hydrogels: DSC, rheological and swelling evidence of a volume phase transition', Polymer Bulletin, 58: 225–234, 2007.

Gruber, H. E., Hoelscher, G. L., Leslie, K., Ingram, J. A., Hanley, E. N., Jr., 'Three-dimensional culture of human disc cells within agarose or a collagen sponge: assessment of proteoglycan production', Biomaterials, 27: 371–376, 2006.

Harley, B. A. C., Hyung-Do, K., Zaman, M. H., Yannas, I. V., Lauffenburger, D. A., Gibson, L. J., 'Microarchitecture of Three-Dimensional Scaffolds Influences Cell Migration Behavior via Junction Interactions', Biophysical Journal, 95: 4013–4024, 2008.

Hasirci, V., Kenar, H., 'Novel surface patterning approaches for tissue engineering and their effect on cell behavior', Nanomedicine, 1: 73-90, 2006.

Hasirci, N., Endogan, T., Vardar, E., Kiziltay, A., Hasirci,V., 'Effect of oxygen plasma on surface properties and biocompatibility of PLGA films', Surface and Interface Analysis, 42: 486 – 491, 2010.

Harnet, E. M., Alderman, J., Wood, T., ‘The surface energy of various biomaterials coated with adhesion molecules used in cell culture’, Colloids and Surfaces B: Biointerfaces, 55: 90–97, 2007.

Haug, A, Smidsrod, O., ‘Effect of divalent metals on properties of alginate solutions. 2. Comparison of different metal ions’, Acta Chemica Scandinavica, 19: 341–351, 1965.

Hermitte, L., Thomas, F., Bougaran, R., Martelet, C., “Contribution of comonomers to bulk and surface properties of methacrylate copolymers”, Journal of Colloid and Interface Science, 272: 82-89, 2004.

Ho, S. T., Hutmacher, D. W., ‘A comparison of micro CT with other techniques used in the characterization of scaffolds’, Biomaterials, 27: 1362–1376, 2006.

Huang, J., Wang X., Yu X., ‘Solute permeation through the polyurethane-NIPAAm hydrogel membranes with various cross-linking densities’, International Congress on Membranes and Membrane Processes, 192: 125-131, 2006.

Inada, Y., Furukawa, M., Sasaki, H., Kodera, Y., Hiroto M., Nishimura, H., Matsushima,A., ‘Biomedical and biotechnological applications of PEG- and PM-modified proteins’, Trends in Biotechnology, 13: 86-91, 1995.

Janvikul, W., Paweena, U., Boonlom, T., Rujiporn, P., Somporn S., ‘Fibroblast interaction with carboxymethylchitosan-based hydrogels’, Journal of Materials Science: Materials in Medicine, 18: 943–949, 2007.

Kaufmann, J., Wiegel, D., Arnold, K., ‘Polar interactions of Hyaluronic acid-Experiments and molecular Dynamics Simulations’, Dispersion Science and Technology, 19: 979-1001, 1998.

Kempen, D.H.R., Lu, L., Hefferan, T.E., Creemers, L.B., Maran, A., Classic, K.L., Dhert, W.J.A., Yaszemski, M.J., Retention of in vitro and in vivo BMP-2 bioactivities in sustained delivery vehicles for bone tissue engineering', Biomaterials, 29: 3245–3252, 2008.

Kim, S. J., Park, S. J., Kim, S. I. 'Swelling behavior of interpenetrating polymer network hydrogels composed of poly(vinyl alcohol) and chitosan', Reactive and Functional Polymers, 55: 53-59, 2003.

Kim, S.S., Gwak, S.J., Kim, B.S., 'Orthotopic bone formation by implantation of apatite-coated poly(lactide-co-glycolide)/hydroxyapatite composite particulates and bone morphogenetic protein-2', Journal of Biomedical Materials Research, 87A: 245-253, 2008.

Kim, J., Yaszemski, M. J., Lu L., 'Three-Dimensional Porous Biodegradable Polymeric Scaffolds Fabricated with Biodegradable Hydrogel Porogens', Tissue Engineering Part C Methods, 15: 583-94, 2009.

Kenar, H., Kose, G. T., Hasirci, V., 'Design of a 3D aligned myocardial tissue construct from biodegradable polyesters', Journal of Materials Science: Materials in Medicine, 21: 989–997, 2010.

Kielty, C. M., Sherratt, M.J., Shuttleworth, C.A. 'Elastic fibres', Journal of Cell Science, 115: 2817–2828, 2002.

Kinikoglu, B., Auxenfansa, C., Pierrillasa, P., Justina, V., Breton, P., Burillond, C., Hasirci, V. and Damour O., 'Reconstruction of a full-thickness collagen-based human oral mucosal equivalent', Biomaterials, 30: 6418-6425, 2009.

Kohn, R., Furda, I., Haug, A., Smidsrod, O., 'Binding of calcium and potassium ions to some polyuronides and monouronates', Acta Chemica Scandinavica, 22: 3098-3102, 1968.

Kosmala, J. D., Henthorn, D. B., Brannon-Peppas, L., ‘Preparation of interpenetrating networks of gelatin and dextran as degradable biomaterials’, Biomaterials, 21: 2019-2023, 2000.

Kulkarni, A. R., Soppimath, K.S., Aminabhavi, T. M., Dave, A. M., Mehta, M. H., ‘Glutaraldehyde crosslinked sodium alginate beads containing liquid pesticide for soil application’, Journal of Controlled Release, 63: 97-105, 2000.

Kumar, N., Langer, R., and Domb, A. “Polyanhydrides: an overview.” Advanced Drug Delivery Reviews, 2002.

Kuo, C. K., Ma, P.X., ‘Ionically crosslinked alginate hydrogels as scaffolds for tissue engineering: part 1. Structure, gelation rate and mechanical properties’, Biomaterials, 22: 511–521, 2001.

Landers, R., Hübner, U., Schmelzeisen, R., Mülhaupt, R., ‘Rapid prototyping of scaffolds derived from thermoreversible hydrogels and tailored for applications in tissue engineering’, Biomaterials 23: 4437–4447, 2002.

Langer, R., Vacanti, J.P., ‘Tissue engineering’, Science 260: 920-926, 1993.

Langer, R., ‘Tissue engineering: a new field and its challenges’, Journal of Pharmarcy Research, 14: 840–841, 1997.

Lauffenburger, D. A., Horwitz, A. F., ‘Cell Migration: A Physically Integrated Molecular Process’, Cell, 84: 359–369, 1996.

Lee, C. H., Singla, A., Lee, Y., ‘Biomedical applications of collagen’, International Journal of Pharmaceutics, 221:1–22, 2001.

Lee, C.R., Grodzinsky, A.J., Spector, M., 'The effects of cross-linking of collagen-glycosaminoglycan scaffolds on compressive stiffness, chondrocyte-mediated contraction, proliferation, and biosynthesis', Biomaterials, 22: 3145–54, 2001.

Lee S. J., Soo K. S., Moo L. Y., 'Interpenetrating polymer network hydrogels based on poly(ethylene glycol) macromer and chitosan', Carbohydrate Polymers, 41: 197–205, 2000.

Levesque, S. G., Lim, R. M., Shoichet, M. S., 'Macroporous interconnected dextran scaffolds of controlled porosity for tissue-engineering applications', Biomaterials, 26: 7436–7446, 2005.

Levental, I., Georgesa, P. C., Janmey, P. A., 'Soft biological materials and their impact on cell function, The Royal Society of Chemistry, 3: 299- 306, 2007.

Liang, S., Xu, J., Weng, L. Dai, H., Zhang, X., Zhang, L., 'Protein diffusion in agarose hydrogel in situ measured by improved refractive index method', Journal of Controlled Release, 115: 189-196, 2006.

Lin, W.C., Yu, D.G., Yang, M.C., 'Blood compatibility of novel poly(γ-glutamic acid)/polyvinyl alcohol hydrogels', Colloids and Surfaces B: Biointerfaces 47: 43-49, 2006.

Lin-Gibson, S., Walls, H. J., Kennedy, B.S., Welsh, E. R., 'Chitosan Hydrogels: Crosslink Kinetics and Gel Properties', Polymeric Materials: Science & Engineering, 88: 199-200, 2003.

Liu Z., 'Calcium-Carboxymethyl Chitosan Hydrogel Beads for Protein Drug Delivery System', Applied Polymer Science, 103: 3164–3168, 2007.

Ma, J., Zhang, Li., Zhen, Li., Borun, L., ‘Preparation and Characterization of Porous Poly (N-isopropylacrylamide)/Clay Nanocomposite Hydrogels’, Polymer Bulletin 61: 593–602, 2008.

Maher, P.S., Keatch, R.P., Donnelly, K., MacKay, R.E., Paxton, J.Z., ‘Construction of 3D biological matrices using rapid prototyping technology’, Rapid Prototyping Journal, 15: 204-210, 2009.

Mahdavinia, G.R., Pourjavadi, A., Hosseinzadeh, H., Zohuriaan, M.J., ‘Modified chitosan 4: Superabsorbent hydrogels from poly(acrylic acid-co-acrylamide) grafted chitosan with salt-and pH-responsiveness properties’, European Polymer Journal, 40: 1399–1407, 2004.

Mandal, B.B., Kundu, S.C., ‘Cell proliferation and migration in silk fibroin 3D scaffolds’, Biomaterials, 15: 2956-65, 2009.

Maldonado-Codina, C., Efron, N., ‘Dynamic wettability of pHEMA-based hydrogel contact lenses’, Opthalmic and Physiological Optics, 26: 408 – 418, 2006.

Mann, B.K., Gobin, A.S., Tsai, A.T., Schmedlen, R.H, West, J.L., ‘Smooth muscle growth in photopolymerized hydrogels with cell adhesive and proteolytically degradable domains: synthetic ECM analogs for tissue engineering’, Biomaterials, 22: 3045–51, 2001.

Marmur, A., ‘Super-hydrophobicity fundamentals: implications to biofouling prevention’, Biofouling, 22: 107–115, 2006.

Matsuyama, A., Tanaka F., ‘Theory of solvation-induced reentrant coil–globule transition of an isolated polymer chain’, Journal of Chemical Physics, 94: 781–786, 1991.

Meena, R., Prasad K., Siddhanta, A.K., ‘Development of a stable hydrogel network based on agar–kappa-carrageenan blend cross-linked with genipin’, Food Hydrocolloids, 23: 497– 509, 2009.

Merrett K., Fagerholm, P., McLaughlin, C. R., Dravida, S., Lagali, N., Shinozaki, N. Watsky, M. A., Munger, R., Kato, Y., Li, F., Marmo, Griffith, C. J. May, ‘Tissue-Engineered Recombinant Human Collagen-Based Corneal Substitutes for Implantation: Performance of Type I versus Type III Collagen’, Investigative Ophthalmology and Visual Science, 49: 3887-3894, 2008.

Mikos, A.G., Sarakinos, G., Leite, S.M., Vacanti, J.P., Langer, R., ‘Laminated three-dimensional biodegradable foams for use in tissue engineering’, Biomaterials, 14: 323-330, 1993.

Moioli, E. K., Clark, P.A., Xin, X., Lal , S., Mao, J. J., ‘Matrices and scaffolds for drug delivery in dental, oral and craniofacial tissue engineering’, Advanced Drug Delivery Reviews, 59: 308-324, 2000.

Mourya, V.K., Inamdar, N., ‘Chitosan-modifications and applications: Opportunities galore’, Reactive & Functional Polymers, 68: 1013–1051, 2008.

Munevar, S., Wang, Y.-L Dembo, M., ‘Distinct roles of frontal and rear cell-substrate adhesions in fibroblast migration’, Molecular Biology of the Cell, 12: 3947-3954, 2001.

Nakamura, K., Murray, R.J., Joseph, J.I., Peppas, N.A., Morishita, M., Lowman, A.M., ‘Oral insulin delivery using P(MAA-g-EG) hydrogels: effects of network morphology on insulin delivery characteristics’, Journal of Controlled Release, 95: 589–599, 2004.

Nayak, S., Debord, S.B., Lyon, L.A., 'Investigations into the deswelling dynamics and thermodynamics of thermoresponsive microgel composite films', Langmuir, 19: 7374–7379, 2003.

Nickerson, M.T., Paulson, A.T., Wagar, E., Farnworth, R., Hodge, S.M., Rousseau, D., 'Some physical properties of crosslinked gelatin–maltodextrin hydrogels', Food Hydrocolloids, 20: 1072-1079, 2006.

Nisbet, D. R., Crompton, K. E., Horne, M. K., Finkelstein, D. I., Forsythe, J. S., 'Neural Tissue Engineering of the CNS Using Hydrogels', Journal Biomedical Material Research Part B: Applied Biomaterials, 87B: 251–263, 2008.

Norotte, C., Marga, F.S., Niklason, L.E., Forgacs, G., 'Scaffold-free vascular tissue engineering using bioprinting', Biomaterials, 30: 5910–5917, 2009.

Novikova, L.N., Mosahebi, A., Wiberg, M., Terenghi, G., Kellerth, J.O., Novikov, L.N. 'Alginate hydrogel and matrigel as potential cell carriers for neurotransplantation', Journal of Biomedical Material Research, 77: 242–252, 2006.

Nunamaker, E. A., Purcell, E. K., Kipke D. R., 'In vivo stability and biocompatibility of implanted calcium alginate disks', Biomedical Materials Research Part A, 83: 1128 – 1137, 2007.

Ono, K., Saito, Y., Yura, H., Ishikawa, K., 'Photocrosslinkable chitosan as a biological adhesive', Biomedical Materials Research, 49: 289–295, 2000.

Oss, C.J., 'Hydrophobicity of biosurfaces-origin, quantitative determination and interaction energies', Journal of Colloids Surface B: Biointerfaces, 5: 91–110, 1995.

Ostrowska-Czubenko, J., Gierszewska-Druzynska, M., 'Effect of ionic crosslinking on the water state in hydrogel chitosan membranes', Carbohydrate Polymers, 77: 590–598, 2009.

Ozcan, C., Hasirci, N., ‘Evaluation of Surface Free Energy for PMMA Films’, Journal of Applied Polymer Science, 108: 438-446, 2008.

Ozcan, C., Hasirci, N., ‘Plasma modification of PMMA films, surface free energy and cell-attachment studies’, Journal of Biomaterials Science Polymer Edition, 18: 759-773, 2007.

Ozcan, C., Zorlutu na, P., Hasirci, V., Hasirci, N., ‘Influence of Oxygen Plasma Modification on Surface Free Energy of PMMA Films and Cell Attachment’, Macromolecular Symposium, 269: 128-137, 2008.

Ozturk, N., Girotti, A., Kose, G.T., Rodriguez-Cabello, J.C., Hasirci V., ‘Dynamic cell culturing and its application to micropatterned, elastin-like protein-modified poly(N-isopropylacrylamide) scaffolds’, Biomaterials 30: 5417–5426, 2009.

Park, K.H, Na, K., Lee, K.C., ‘Immobilization of Arg-Gly-Asp (RGD) sequence in sugar containing copolymer for culturing of pheochromocytoma (PC12) cells’, Journal of Bioscience Bioengineering, 97: 207–211, 2004.

Park, H., Kang. S., Kim, B.S., Mooney, D. J., Lee, K. Y., ‘Shear-reversibly Crosslinked Alginate Hydrogels for Tissue Engineering’, Macromolecular Bioscience, 9: 895–890, 2009.

Park, S.N, Park, J.C., Kim, H.O., Song, M.J., Suh, H., ‘Characterization of porous collage/hyaluronic acid scaffold modified by 1- ethyl-3-(3-dimethylaminopropyl) carbodiimide cross-linking’, Biomaterials, 23: 1205–12, 2002.

Parks, W.C., Pierce, R.A., Lee, K.A., Mecham, R.P., ‘Elastin’, Advanced Molecular Cellular Biology, 6: 133–182, 1993.

Pelham, R.J., Wang, Y., ‘Cell locomotion and focal adhesions are regulated by substrate flexibility’, Proceedings of the National Academy Science, 94: 13661–13665, 1997.

Pfister, P.M, Wendlandt, M., Neuenschwander, P., Suter, U.W, ‘Surface-textured PEG-based hydrogels with adjustable elasticity: Synthesis and characterization’, Biomaterials, 28: 567, 2007.

Pfister, L.A., Alther, E., Papaloïzos, M., Merkle H.P., Gander, B., ‘Controlled nerve growth factor release from multi-ply alginate/chitosan-based nerve conduits’, European Journal of Pharmaceutics and Biopharmaceutics, 69: 563–572, 2008.

Pourjavadi, A, Kurdtabar, M., ‘Effect of different bases and neutralization steps on porosity and properties of collagen-based hydrogels’, Polymer International, 59: 36–42, 2010.

Prabaharan, M., Mano, J. F., ‘Chitosan-Based Particles as Controlled Drug Delivery Systems’, Drug Delivery, 12: 41-57, 2004.

Ramakrishna, S., Mayer, J., Wintermantel, E., Kam, Leong W., ‘Biomedical applications of polymer-composite materials: a review’, Composites Science and Technology, 61: 1189-1224, 2001.

Rees, D.A., Steele, I.W. and Williamson, F.B, ‘Conformational analysis of polysaccharides’, Journal Polymer Science, 28: 261, 1969.

Rees, D., Welsh, E. Angew, J., ‘Secondary and Tertiary Structure of Polysaccharides in Solutions and Gels’, Chemistry International Edition England, 16: 214-224, 1977.

Revell, C. M., Athanasiou, K.A., ‘Success Rates and Immunologic Responses of Autogenic, Allogenic, and Xenogenic Treatments to Repair Articular Cartilage Defects’, Tissue Engineering Part B: Reviews, 15: 1-15, 2009.

Ridley, A. J., Schwartz, M. A., Burridge, K., Firtel, R. A., Ginsberg, M. H., Borisy, G., Parsons, J. T., Horwitz, A.R., ‘Cell Migration: Integrating Signals from Front to Back’, Science, 302: 1704-1709, 2003.

Rinaudo, M., ‘Main properties and current applications of some polysaccharides as biomaterials’, Polymer International, 57: 397–430, 2008.

Rohanizadeh, R., Swain, M.V., Mason, R.S. ‘Gelatin sponges (Gelfoam®) as a scaffold for osteoblasts’, Journal of Materials Science: Material Medicine, 19: 1173–1182, 2008.

Rosiak J. M., Yoshii F., ‘Hydrogels and their medical applications’, Nuclear Instruments and Methods in Physics Research B, 151: 56-64, 1999.

Rowley, J. A., Madlambayan, G., Mooney, D. J., ‘Alginate hydrogels as synthetic extracellular matrix materials’, Biomaterials, 20: 45-53, 1999.

Sakai, S., Hashimoto I., Kawakami, K., ‘Agarose–gelatin conjugate for adherent cell-enclosing capsules’, Biotechnology Letters, 29: 731–735, 2007.

Sarasam, A.R., Brown, P., Khajotia, S.S., Dmytryk, J.J., Madihally, S.V. ‘Antibacterial activity of chitosan-based matrices on oral pathogens’, Journal of Materials Science: Materials in Medicine, 19: 1083-1090, 2008.

Schulz, R., Höhle, S., Zernia, G., Zscharnack, M., Schiller, J., Bader, A., Arnold, K., Huster, D., ‘Analysis of Extracellular Matrix Production in Artificial Cartilage Constructs by Histology’, Immunocytochemistry, Mass Spectrometry, and NMR Spectroscopy, Nanoscience and Nanotechnology, 6: 1–14, 2006.

Schmedlen, R. H., Masters, K. S., West J. L., ‘Photocrosslinkable polyvinyl alcohol hydrogels that can be modified with cell adhesion peptides for use in tissue engineering’, Biomaterials, 23: 4325–4332, 2002.

Schneider, G. B., English, A., Abraham M., Zaharias, R., Clark S., Keller, J., ‘The effect of hydrogel charge density on cell attachment’, Biomaterials, 25: 3023–3028, 2004.

Schweitzer, S.K., Habib, M., Gepstein, L., Seliktar, D., ‘A photopolymerizable hydrogel for 3-D culture of human embryonic stem cell-derived cardiomyocytes and rat neonatal cardiac cells’, Molecular and Cellular Cardiology, 46: 213–224, 2009.

Schugens, C, Maquet, V., Grandfils, C, Jerome, R., Teyssie, P., Journal of Biomedical Materials Research, 30: 449, 1996.

Schliephake H, Neukam FW and Kolsa D, International Journal of Oral Maxillofacial Surgery, 1991.

Se, H.O., Soung, G.K., Jin, H.L., ‘Degradation behavior of hydrophilized PLGA scaffolds prepared by melt-molding particulate-leaching method: Comparison with control hydrophobic one’, Journal of Material Science Materials in Medicine, 17: 131-137, 2006.

Sen, Murat, Avcı, E. N., ‘Radiation synthesis of poly(N-vinyl-2-pyrrolidone)-carrageenan hydrogels and their use in wound dressing applications. I. Preliminary laboratory tests’, Journal of Biomedical Materials Research, 7: 187-196, 2005.

Serra, L., Doménech, J., Peppas, N. A., ‘Engineering design and molecular dynamics of mucoadhesive drug delivery systems as targeting agents’, European Journal of Pharmaceutics and Biopharmaceutics, 71: 519–528, 2009.

Sharma, R., Greenhough, S., Medine, C. N., Hay, D. C., 'Three-Dimensional Culture of Human Embryonic Stem Cell Derived Hepatic Endoderm and Its Role in Bioartificial Liver Construction', Biomedicine and Biotechnology, 2010, Article in press.

Sheikh, N., Jalil, L., Anvari, F., 'A study on the swelling behavior of poly(acrylicacid) hydrogels obtained by electron beam crosslinking', Radiation Physics and Chemistry, 79: 735-739, 2010.

Silva, A. K., Richard, C., Bessodes, M., Scherman, D., Merten, Otto-Wilhelm, 'Growth Factor Delivery Approaches in Hydrogels', Biomacromolecules, 10: 9–18, 2009.

Simonid, L.J.T., Maja, M., Jovanka, M. F., Suljovrujic, E. H., 'Swelling and thermodynamic studies of temperature responsive 2-hydroxyethyl methacrylate/itaconic acid copolymeric hydrogels prepared via gamma radiation', Radiation Physics and Chemistry, 76: 1390–1394, 2007.

Studenovska, H., Miroslav, S. Frantisek, R., 'Poly(HEMA) hydrogels with controlled pore architecture for tissue regeneration applications', Journal of Materials Science: Materials in Medicine, 19: 615–621, 2008.

Tamada, J. and Langer, R. "The development of polyanhydrides for drug delivery applications." Journal of Biomaterials Science, Polymer Edition, 3:315–353, 1992.

Tan, G., Wang, Y., Li, J., Zhang, S., 'Synthesis and Characterization of Injectable Photocrosslinking Poly (ethylene glycol) Diacrylate based Hydrogels', Polymer Bulletin, 61: 91–98, 2008.

Tessmar, J. K., Gopferich, A. M., 'Customized PEG-derived copolymers for tissue-engineering applications', Macromolecular Bioscience, 7: 23-39, 2007.

Tian, H., Shantaram, B., Yan, L., Mab, H., Ma, P. X., Atala, A., Zhang, Y., 'Myogenic differentiation of human bone marrow mesenchymal stem cells on a 3D nano fibrous scaffold for bladder tissue engineering', Biomaterials, 31: 870–877, 2010.

Tsourapas, G., Rutten, F.J.M., Briggs, D., Davies, M.C., Shakesheff K.M., 'Surface spectroscopic imaging of PEG-PLA tissue engineering constructs with ToF-SIMS', Applied Surface Science, 252: 6693–6696, 2006.

Tunc, Y., Hasirci, N., Yesilada, A., Ulubayram, K., 'Comonomer effects on binding performances and morphology of acrylate-based imprinted polymers', Polymer, 47: 6931-6940, 2006.

Tønnesen, H. H., Karlsen, J., 'Alginate in Drug Delivery Systems', 28: 621-630, Drug Development and Industrial Pharmacy, 2002.

Ulubayram, K., Kiziltay, A., Yilmaz, E., Hasirci, N., 'Desferrioxamine release from gelatin-based systems', Biotechnology and Applied Biochemistry, 42: 237-245, 2005.

Vieira, E., 'Polysaccharide-Based Hydrogels: Preparation, Characterization, and Drug Interaction Behaviour', Biomacromolecules, 9: 1195–1199, 2008.

Vogt, S., Larcher, Y., Beer, B., Wilke, Schnabelrauch, I. M. 'Fabrication of Highly porous scaffold materials based on functionalized oligolactides and Preliminary results on their use in bone tissue Engineering', European Cell and Materials, 4: 30-38, 2002.

Wan Y., X. Qu, J. Lu, C. Zhu, L. Wan, J. Yang, J. Bei, S. Wang, Biomaterials, 25: 4777, 2004.

Wang, T., Gunasekaran, S., ‘State of Water in Chitosan–PVA Hydrogel’, Applied Polymer Science, 101: 3227–3232, 2006.

Wang, Y., Kim, H. J., Vunjak-Novakovic, G., Kaplan, D. L., ‘Stem cell-based tissue engineering with silk biomaterials’ Biomaterials, 27: 6064-6082, 2006.

Wang, Z.C., X.D., Chen, C.S. Wang, G.R., Zhan, X.Z., Zhuo, R.X., ‘Study on novel hydrogels based on thermosensitive PNIPAAm with pH sensitive PDMAEMA grafts’, Colloids and Surfaces B: Biointerfaces, 67: 245–252, 2008.

Wang, Y. Q., Cai, ‘Enhanced cell affinity of poly(l-lactic acid) modified by base hydrolysis: Wettability and surface roughness at nanometer scale’, Journal of Current Applied Physics, 7: 108, 2007.

Wang, Y., Yin, S., Ren, L., Zhao, L. ‘Surface characterization of the chitosan membrane after oxygen plasma treatment and its aging effect’, Biomedical Materials, 4: 1-7, 2009.

West, E. R., Xu, M., Woodruf, T. K., Sheaa, L.D., ‘Physical properties of alginate hydrogels and their effects on in vitro follicle development’, Biomaterials, 28: 4439–4448, 2007.

Whang, K., Thomas C.K., Nuber G., Healy K.E., ‘A novel method to fabricate bioresorbable scaffolds’, Polymer, 4: 837-842, 1995.

Wiegand, C., Hipler, U.C., ‘Evaluation of Biocompatibility and Cytotoxicity Using Keratinocyte and Fibroblast Cultures’, Skin Pharmacology Physiology, 22: 74-82, 2009.

Wiegel, D., J. Kaufmann, Arnold K., ‘Polar interactions of chondroitinsulfate, Surface free energy and molecular dynamics simulations’, Colloids and Surfaces B: Biointerfaces, 13: 143–156, 1999.

Willerth, S. M., Sakiyama-Elbert, S. E., ‘Approaches to Neural Tissue Engineering Using Scaffolds for Drug Delivery’, Advanced Drug Delivery Revision, 30: 325–338, 2007.

Witcherle O., Lim D., ‘Hydrophilic gels for biological use’, Nature, 185: 117-118, 1960.

Woźniak, P., Kozicki, M., Rosiak, J. M., Przybylski, J., Szumieł, M. L., ‘Alginate hydrogel-candidate support for cell transplantation-preliminary observation in human chondrocyte culture’, Drug Dev Ind Pharm., 28: 621-30, 2002.

Woerly, S., ‘Restorative surgery of the central nervous system by means of tissue engineering using NeuroGel implants’, Neurosurgical Revision, 23: 59–77, 2000.

Yanpeng, J., Zonghua, L., Shan, D., Lihuo, L., Changren, Z. ‘Preparation of biodegradable crosslinking agents and application in PVP hydrogel’, Applied Polymer Science, 10: 1515-1521, 2006.

Yeong, W. Y. Chua, C. K. Leong, K. F. Chandrasekaran, M. ‘Rapid prototyping in tissue engineering: challenges and potential’, Trends Biotechnology, 22: 643–652, 2004.

Yilgor, P., Sousa, R.A., Reis, R.L., Hasirci, N., Hasirci, V., ‘3D Plotted PCL Scaffolds for Stem Cell Based Bone Tissue Engineering’, Macromolecular Symposia, 269: 92-99, 2008.

Yilgor P., Tuzlakoglu, K., Reis, R.L. Hasirci, N., Hasirci, V., 'Incorporation of a Sequential BMP-2/BMP-7 Delivery System into Chitosan-Based Scaffolds for Bone Tissue Engineering', Biomaterials, 30: 3551-3559, 2009.

Yu, T.T, Shoichet, M.S., 'Guided cell adhesion and outgrowth in peptide-modified channels for neural tissue engineering', Biomaterials, 26: 1507–1514, 2005.

Yucel, D., Kose, G. Hasirci, V., 'Polyester based nerve guidance conduit design', Biomaterials, 31: 1596-1603, 2010.

Zan, J., Chen, H., Jiang, G., Lin, Y., Ding, F., 'Preparation and Properties of Crosslinked Chitosan Thermosensitive Hydrogel for Injectable Drug Delivery Systems', Journal of Applied Polymer Science, 101: 1892–1898, 2006.

Zhang, X., Zhuo, R., Yang, Y., 'Using mixed solvent to synthesize temperature sensitive poly(N-isopropylacrylamide) gel with rapid dynamics properties', Biomaterials, 23: 1313–1318, 2002.

Zhao, Q., Sun, J., Ling Q., Zhou, Q., 'Synthesis of Macroporous Thermosensitive Hydrogels: A Novel Method of Controlling Pore Size', Langmui, 25: 3249-3254, 2009

Zivanovic,, S., Li, J., Davidson, P.M., Kit, K., 'Physical, Mechanical and Antibacterial Properties of Chitosan/PEO Blend Films'. Biomacromolecules, 8: 1505-1510, 2007.

Zonghua, L., Yanpeng, J., Zhang Z., 'Calcium-Carboxymethyl Chitosan Hydrogel Beads for Protein Drug Delivery System', Applied Polymer Science, 103: 3164–3168, 2007.